

## **Responses to comments of Anonymous Referee #1**

We thank anonymous referee #1 for reviewing our manuscript and considering our manuscript suitable for publication in ACP after minor revision. Please find below our detailed response to the comments.

### **General Comments:**

The referee #1 has recommend language revision for the manuscript.

Response: We highly appreciate Referee #1's suggestion and efforts in providing list of grammatical corrections. In the revised manuscript we have taken all the possible care besides including corrections suggested by the reviewer. In addition, the manuscript will go through language editing by professional language editor before being published in ACP.

### **Specific Comments:**

*(1) p. 15795: In the description of the NARL lidar the orthogonal aligned PMT are mentioned. This sounds like the NARL lidar is able to measure the depolarization of particles. If so, why not using the depolarization data as indicator for ice clouds?*

Response: Though the NARL lidar has orthogonally aligned PMTs and hence the ability to measure depolarization of particles, during many years the depolarization measurements were not made. Hence, the use of depolarization as an indicator of ice-clouds would have significantly reduced the number of profiles available for cirrus cloud climatology. So, for uniformity and continuity, we have chosen temperature as a parameter to distinguish cirrus clouds from water clouds.

*(2) p. 15798 Section 3.1: In this Section the cloud detection algorithm is described briefly. You state that the algorithm is optimized to detect very thin clouds. Can you please provide some numbers, what is the smallest/ thinnest cloud with respect to vertical and spatial extent you could detect with the algorithm. This numbers should also stated for CALIPSO, as they are quite important for comparing numbers/frequencies of thin clouds. Are you applying any additional profile smoothing in time or vertical ? How sensitive is the detection algorithm with respect to noise in the backscatter profiles ?*

Response: Our cloud detection algorithm is based on wavelet covariance transform (WCT) method using Haar wavelet. The algorithm is able to detect clouds which have geometrical thickness greater than or equal to 600 m (two altitude bins). While no smoothing along vertical direction is applied to raw profiles, use of dilation value equal to 3 in the WCT algorithm has effect somewhat similar to 2 point smoothing. Individual raw profile is a time integration of four minutes of data acquisition. The algorithm uses a threshold in transformed profile for detecting the cloud layers. The threshold value is a linear function of altitude. Altitude varying threshold has benefit of low noise in near range and avoids false detection at the far end. In addition, each LIDAR profile (clear/cloudy) before being considered for inclusion undergoes quality check based on signal to noise ratio (SNR) at 5 km and 20 km altitude bins. Only those LIDAR profiles which had SNR greater than 1000 at 5 km and SNR

greater than 10 at 20 km are used in the analysis. Also, to avoid false detection for noisy data, if the detected cloud layer has peak photon counts less than background plus 3 x std then they are not considered. Though CALIOP profiles have vertical resolution of 60 m, the lowest geometrical thickness of clouds that we could find in the data-set used in current study is 360 m. This information is included in the revised manuscript.

*(3) p. 15798 ll 8: You considered only those clouds with a base temperature of below -20 °C. Would it be better to use a temperature of -38°C (235 K) for classification of cirrus layer, since below this temperature liquid cloud droplets no longer form. The temperature range between -38°C - 0°C is assigned to mixed phase clouds where the coexistence of water droplets and ice particles typically occur. The ice water content as well as the optical depth in such even though completely frozen clouds is much higher compared to real cirrus clouds found in temperatures below -38°C. How would your results change, if you take only those clouds below -38°C which are then most certainly cirrus clouds?*

Response: We agree with the concern of the referee that use of temperature range -20 to -38 °C may result in misclassification of few mixed phase clouds as cirrus clouds. However, equally valid argument may have been raised that we may under-sample cirrus clouds if we would have used “< -38 °C” as cirrus cloud criteria. Cirrus clouds also form at warmer temperatures (greater than -38°C) through one or two heterogeneous freezing mechanisms (Lynch et al., 2002; Cziczo and Froyd, 2014). Moreover, cirrus clouds formed at higher altitudes (lower temperatures) many times gradually descend down to lower altitudes (higher temperatures) due to the sedimentation of ice-crystals. We have considered all the cloud layers below -20°C as cirrus layers. In case of ground-based observations (NARL lidar), the observations were carried out only when low level clouds were not present (to prevent the saturation of PMT due to very strong backscatter from the deep convective clouds/water clouds where particles are in mixed phase and to avoid accidental exposure of system to rain water). In absence of big convective system, chance of having mixed phase clouds is small. Using < -38°C as criteria may not have much bearing on trend analysis as we see that statistically significant trends are found only for sub-visible cirrus clouds which form at ultra low temperature. The mean, median and standard deviation of the various cirrus cloud properties shown in Table 3 change slightly when we take only those clouds below -38°C (see the table below). The histograms shown in Figure 4 will become slightly sharper if this criterion is chosen.

**Table2: Cirrus properties for cirrus clouds below -38 °C.**

Cirrus cloud properties	NARL Lidar	CALIOP (night)	CALIOP (day)
Base altitude (km)	13.5±1.8 (13.4)	13.6±1.6 (13.6)	13.5±1.5 (13.3)
Top altitude (km)	15.7±1.6 (15.8)	15.5±1.6 (15.9)	15.1±1.5 (15.4)
Mid-cloud altitude (km)	14.6±1.6 (14.6)	14.6 ± 1.5 (14.7)	14.3±1.4 (14.2)
Geometrical thickness (km)	2.2±1.2 (1.8)	2.0±1.3 (1.6)	1.6±1.1 (1.2)
Mid-cloud temperature (°C)	-68.1±8.6 (-69.8)	-67.5±10.1 (-69.6)	-65.7±9.9 (-66.9)

Distance from tropopause (km)	-2.1±1.7 (-2.1)	-2.0±1.5 (-1.7)	-2.2±1.5 (-2.0)
-------------------------------	-----------------	-----------------	-----------------

*(4) p. 15799 ll 22-25: As you wrote before, multiple scattering is important to consider. Why do you use different multiple scattering correction factors (0.75 and 0.6) for the NARL and CALIPSO extinction retrieval ? The correction factor depends strongly on the Field of View (FOV) of the lidar receiver. Does NARL have a similar FOV as Sassen Cho (1992) used in their study or why did you chose the same correction factor ?*

Response: Sassen & Comstock (2001) used multiple scattering factor,  $\eta=0.6$  to  $0.7$  for optically thick clouds,  $\eta=0.8$  for thin cirrus and  $\eta=0.9$  for sub-visible cirrus clouds. Instead of variable multiple scattering factor, we have selected an intermediate value  $0.75$  for all cloud types. The field of view (FoV) of NARL lidar ( $1$  mrad) and the lidar system ( $3$  mrad) used by Sassen & Cho (1992) is comparable. Value of  $\eta$  affects the magnitude of estimated cloud optical depth. In our manuscript we have reported that NARL lidar detects more sub-visible cirrus clouds than CALIOP. If we would have used  $\eta=0.6$  instead of  $0.75$  then the difference between the two would have been even larger. In other words while we do not find strong justification to use  $0.6$  value for  $\eta$ , use of value  $0.75$  is not affecting one of our major conclusion. In the revised manuscript, we have included justification for our choice of multiple scattering correction factor.

*(5) p. 15801 ll 14-15: You mentioned the quite large difference between CALIOP and NARL PO distribution and explained it with occurrence of cloudy nights during the monsoon season. However, Figure 2d shows no significant difference between CALIPSO and NARL PO distribution during the monsoon season in order that this may not be the right reason for the difference. Except for the post-monsoon season all PO distributions from the NARL lidar appear to be comparable with CALIOP. For combining Figures 2b-e into the Figure 2a it seems that the most of the data are collected during Post-monsoon season. That brings me to the question of how many profiles are used for each season for CALIOP and NARL? Another reason for the difference could be attributed to different bin-width in determining the PO distribution for the CALIOP and the NARL lidar. Are you using the same bin-width for the NARL and CALIOP PO distribution ?*

Reply: \_

Please note that the range of X-axes in Fig 2b to 2e is twice that of used in Fig 2a. Hence, differences between NARL lidar and CALIOP appear smaller in seasonal PO distributions. Total number of profiles measured and number of profiles with presence of clouds are shown in the table below. Since no weighting is applied for the differences in total number of profile available in different seasons, the mean PO distribution shown in Fig 2a is dominated by the season when large number of measurements were carried out. In case of NARL lidar winter and pre-monsoon are the seasons when more number of lidar measurements were made but these two are also the seasons when cloud fraction is low. In case of CALIOP, nearly same number of profiles are available in each season.

In the second part of the question, reviewer has asked whether we used same bin-width for NARL lidar and CALIOP. NARL Lidar has range resolution of  $300\text{m}$  whereas CALIOP has range resolution  $60\text{m}$ . To find out whether the difference in range resolution will have effect on PO distribution, we have carried-out sensitivity tests. We reduced CALIOP data to coarser

resolutions like 120m, 240m, 300m and 600m by averaging and recalculated PO values. Effect of increasing bin-width is found to result in small increase in PO (less than 5% at 300m). This is because as we reduce the resolution, cloud presence spills to neighbouring bins which otherwise would have been counted as cloud free bins. Following table will be provided as supporting material.

Seasons	NARL Lidar		CALIOP	
	Total no. of profiles	Total no. of cloudy profiles	Total no. of profiles	Total no. of cloudy profiles
Winter (DJF)	41205	13515	720 (673)*	298 (218)
Pre-monsoon (MAM)	28695	13140	741 (674)	385 (334)
Monsoon (JJA)	9090	6900	781 (780)	698 (680)
Post-monsoon (SON)	14700	7725	780 (779)	495 (588)
Total	93690	41280	3022 (2906)	1876 (1820)

(\* Value in the parentheses corresponds to CALIOP day-time observations.)

*(6) p. 15803 ll 10-16: The day night time difference in PO depends strongly on the amount of CALIOP profiles. How significant are these differences, especially the slightly larger day-time PO during September and November ?? Can state some explanation, why the day-time PO could be larger compared to the night-time PO?*

**Reply:** Number of total profiles available during day and night are not significantly different. This can be seen in the table provided in response to previous comment. In response to this comment, we carried out Student's T-test on day-night differences and found that the differences are not statistically significant. This is because we have chosen relatively small domain around Gadanki where number of overpasses and hence the available profiles is small. Since, the difference is not statistically significant, we have decided to drop the Fig 3c and 3d from revised manuscript.

*(7) p. 15804 ll 20-21: "Quite a good number", can you please state a percentage number for NARL and also for CALIPSO. Did you checked the differences in the FNL and GMAO tropopause heights as well as the temperature data ?*

**Reply:** We have found that on average FNL tropopause height is 16.559 km and GMAO tropopause height is 16.596 km which are very close. About 9% of the clouds were found above the tropopause in case of NARL Lidar. We have included this information in the revised manuscript.

*(8) p. 15804 ll 24-25: Is there an explanation for the noticeable peak at -75\_C in the NARL mid-cloud temperature ?*

**Reply:** Both the lidars (CALIOP and NARL) have peak of frequency distribution at -75 deg C. However the peak is prominent in case of NARL Lidar. This is possibly due to fact that NARL Lidar detects more number of sub-visible cirrus clouds which are found to occur more frequently at temperature -75 deg C (see Fig. 10 of our manuscript). Also, the tropopause which is at approximately 16 km acts as cap for cloud top. With average cloud thickness of the order 2 km, cloud mid-altitude will be located at 15 km which corresponds to -75 C°.

*(9) p. 15804 ll 26-28: Can please state the percentage of sub-visible, thin and thick cirrus clouds also in the respective panel of Figure 6 (b-d) as text. Than it is easier to understand the composition of panel a.*

**Reply:** We agree with reviewer's suggestion. In the revised manuscript, we state the percentage of sub-visible, thin and thick cirrus clouds in the respective panel of Figure 6 (b-d) as text.

*(10) p. 15807 ll 19-22: Is there an explanation why CALIPSO underestimates the thickness in day-time profiles ?*

**Reply:** Thorsen et al. (2013) have considered high noise level in day-time lidar profiles as a reason for underestimation of cloud thickness during day by CALIOP. The background noise in CALIOP data during day time increases by factor of 10. The high background level makes it difficult to detect tenuous cloud top and base which results in overall smaller geometrical thickness. They arrived on this conclusion based on comparison with Raman lidar which has low background noise during day and does not have statistically significant difference in day and night thickness of clouds at Darwin, Australia. We have included this information in the revised manuscript.

*(11) p. 15808 ll 9-13: This point is very unclear and needs further explanation: The difference in geometrical thickness between Sunilkumar and Parameswaran (2005) and your study can be hardly explained by different temperature data. The geometrical thickness measurement itself does not depend on temperature due to the good resolution of a lidar. Only the individual cloud thickness could be shifted to other temperature bins, but this would require a temperature difference between both datasets of more than 20K to explain the big difference of temperature / geometrical thickness distribution.*

**Reply:** We agree with the referee that the differences in temperature profiles alone are not sufficient to explain the observed difference between our results and that of Sunil Kumar and Parameswaran (2005). Other factors such as size of data set, differences in cloud detection algorithm, etc. can also contribute to the observed differences. In the revised manuscript, we have included this caveat to our explanation.

*(12) p. 15808 ll 15-17: The dependence could be weaker, but as you wrote before (p. 15807 ll 19-22) the cloud thickness in CALIPSO day-time profiles could also be underestimated. I think this needs a bit more discussion what is the reason for the day/night time difference.*

**Reply:** Yes, we agree with the referee's point that the weaker dependence could be due to the underestimation of geometrical thickness of clouds. We have added statement that the weaker dependence could be due to underestimation of cloud thickness during day-time by CALIOP in the revised manuscript.

*(13) p. 15810 l 2: Can you please state the trend of decreasing optical thickness of thick cirrus clouds in the text. Maybe it is also helpful, to show this significant trend also in a Figure.*

**Reply:** As suggested by the review we have added the trend of the optical thickness of thick cirrus clouds in the text, also we have included figure with trend analysis for thick cirrus clouds in the supporting material.

*(14) p. 15810 l 12-15: This statement needs clarification, because the intention is not clear and the arguments are contradictory. First you wrote that there is a warming trend at 100 hPa. In the next sentence you wrote the warming decreases rapidly and becomes*

**Reply:** In this statement we mean to say that CMIP5 projections showed a warming trend at 100 hPa over the wide region of 60°N to 45°S. However, this warming trend decreases rapidly and becomes cooling with increase in altitudes. At 100 hPa the temperature increases by ~3.27 K at the end of twenty-first century and at 10 hPa, the temperature decreases by ~8.8 K at the end of twenty-first century. We have changed the statement in revised manuscript to avoid confusion.

*(15) p. 15811 l 3-5: Can you please state a percentage number also in the conclusion section. Because it is an important point for water vapor entry into the TTL.*

**Reply:** Number of cirrus clouds above tropopause is found to be 9% in NARL lidar. This is mentioned in the revised manuscript.

*(16) p. 15811 l 8-11: As i mentioned before, i did not understand the difference in the Temperature/Thickness distribution and the corresponding explanation.*

**Reply:** See our response to comment 11.

### **3 Technical comments:**

We agree with all the technical corrections and implemented them in the revised manuscript except two suggestions which were about improving readability of Fig. 1 and 6. Our software does not support suggested correction, hence we are looking for alternative software. If necessary we will be doing that at later stage (proof reading stage).

### **References:**

Cziczo, D.J. and Fryod, K.D.: Sampling the composition of cirrus ice residuals, Atmospheric Research, 142, 15–31,

Lynch, D. K., Sassen, K., Starr, D., and Stephens, G. (Eds.): Cirrus, Oxford University Press, New York, USA, 499 pp., 2002.

## **Responses to comments of Anonymous Referee #2**

We thank anonymous referee #2 for reviewing our manuscript and emphasising the fact that manuscript is a work based on a unique dataset from a region which is under-represented in terms of long-term cloud observations. We thank referee #2 for considering our manuscript suitable for publication in ACP after minor revision. Please find below our detailed response to the comments.

### **Specific Comments**

*1. Abstract and Title: The abstract and title mainly reflect the climatology portion of the work, which is the bulk of what is presented. But the trend analysis is also important and suggest you add specific language in the abstract about the magnitude of the trends and their link to signatures of climate change. Also, you modify the title to draw some attention to the work. Suggest “Long-term trend analysis and climatology of tropical cirrus clouds using 16-yr lidar dataset over southern India” or something similar.*

**Reply:** We thank the referee for suggesting this improvement. In the revised manuscript, we are changing title as suggested by the referee. We have also modified the abstract to give more emphasis on long-term trend analysis.

*2. P. 15800, Line 14: “Data product is known as: : :” suggest “We use the feature optical depth data product from the CALIOP level-2 data product.”*

**Reply:** As suggested by the referee we have modified the sentence in the revised manuscript.

*3. In many places you discuss the differences in cloud thickness or altitude between the two datasets, but you do not consider the differences in vertical resolution of the two lidar systems as a possible source of the discrepancies. This needs to be discussed in many instances. You could start with a discussion in the methodology section about the relative sensitivity of the two lidar systems (i.e. signal to noise ratio) and the vertical resolution differences. You mention a 5 km CALIOP cloud layer product. This is very large! For NARL you state 300 m. This is a big discrepancy. Please address how you handled these differences in your analysis.*

**Reply:** In this context, the 5 km CALIOP cloud layer product implies horizontal resolution of 5 km along the track of satellite. The vertical resolution of CALIOP data is 60 m. The vertical resolution of NARL lidar is 300 m. The details of vertical resolution of both Lidars is provided in Table 1. In the revised manuscript, we include this information in text also.

*4. Discussion on P. 15801 and 15802, Frequency and maintenance of tropical tropopause layer (TTL) cirrus clouds: You state that the formation of cirrus clouds in the tropics is due to deep convective clouds. Yes, this is true for some tropical cirrus, but the TTL cirrus is not necessarily formed by deep convection, but can be the result of stratospheric waves (Boehm et al.) or can self maintain for up to 2 days through cloud radiative heating processes (Dinh, et al. 2010). You need to consider these studies in your discussion. TTL cirrus can last for days and has been shown to do so by many.*

*If there is a discrepancy between day and night time TTL cirrus occurrence, then it is due to instrument sensitivity during the daytime. Please address these issues more quantitatively in the discussion of the results.*

Reply: We agree that there are several mechanisms through which TTL cirrus cloud can form. However, other mechanism such as suggested by Boehm et al. (2000) or Dinh et al (2010) cannot account for day and night difference. A related comment is received by referee #1 asking to perform significance test for the monthly differences between day and night percentage of occurrence. We found that the monthly differences are not statistically significant due to small data-set available in the region 50 km around Gadanki. Hence in the revised manuscript we are reducing the discussion about day and night differences particularly which is based on Fig. 3.

*5. Last sentence of Sec. 4.1: This statement should be removed because it is not a legitimate physical difference but an artifact of the instrument.*

Reply: As mentioned in the previous comment, we are going to reduce all the discussion about day-night difference including the statement mentioned here.

*6. Again on p. 15803 Lines 13-15: we can't definitely conclude that the day-night differences are a real atmospheric phenomenon because of the instrument issues.*

Reply: Please see our response to previous comment.

*7. P. 15804: The tropical tropopause is not well defined. How are you identifying the tropopause?*

Reply: We used cold-point tropopause definition to calculate tropopause height from temperature profiles of FNL. However, in the revised manuscript we have decided to use tropopause altitude provided as a part of FNL data which uses lapse rate tropopause definition. We find no significant difference in the percentage of occurrence of cirrus clouds above tropopause in NARL lidar data, nevertheless we made this decision as tropopause height provided part of FNL data is a standard product and its comparisons with similar products from other datasets are available in literature e.g. Pan and Munchak (2011).

*8. P. 15805, lines 10-15: Could this discrepancy be the vertical resolution or sensitivity issue?*

Reply: We believe that NARL lidar has better sensitivity than CALIOP which is responsible for more detection of sub-visible cirrus than CALIOP. CALIOP has 60 m vertical resolution whereas NARL lidar has 300 m vertical resolution. We carried out sensitivity study to investigate the effects of bin-width on PO distribution by rebining CALIOP data at coarser resolutions and found no significant difference in PO distributions at 60m and 300m resolutions. Though, we found vertical resolution not playing direct role, indirectly high vertical resolution can reduce the signal strength and hence increase the signal to noise ratio. The sensitivity issue of CALIOP lidar is also pointed out by other researchers like Davis et al., 2010, Martins et al., 2011, Thorsen et al., 2013, etc.

*9. P. 15806: How accurate are the NARL optical depths <0.01? what is the uncertainty?*



Reply: Since no standards are available to compare against, we used estimates of errors in inputs and their propagation to compute cloud optical depth for determining precision and accuracy of NARL lidar. From error analysis, we found that the NARL lidar can estimate cloud optical thickness with precision of the order of  $10^{-4}$ . However, the precision should not be confused with accuracy which is largely determined by accuracy of assumptions as mentioned next. The largest sources of errors are lidar-ratio (extinction to backscatter ratio) and multiple scattering correction factor ( $\eta$ ). Effect of lidar-ratio and  $\eta$  on output values (extinction coefficient or optical depth) is similar to scaling the output values with these parameters. The lidar ratio and  $\eta$  values being used in current study are expected to have about 20% error based on the values reported in literature. Both the parameters together will contribute about 40% error in the cloud optical thickness.

*10. P. 15807, Lines 20-22: I believe this is an instrument detection issue in daytime coupled with vertical resolution.*

Reply: We agree with the referee's suggestion. The statement is changed to reflect this caveat.

*11. P. 15808, last paragraph: you should acknowledge the reasons for the differences in cloud properties in these temperature regimes is due different cloud formation mechanisms.*

*See (4) above.*

Reply: As suggested by the reviewer, we included the reasons for the differences in the clouds properties in these temperature regimes in the revised text.

*12. P. 15809, line 15-16: Why not use cloud top temperature for this analysis? Midcloud height has thickness and cloud altitude influences. Cloud top altitude would be the trend in altitude alone. Are the trends robust for cloud top temperature? Please add to the discussion.*

Reply: After receiving the reviewer's suggestion we analysed trends in temperature at cloud-top and found the trend of  $0.02 \pm 0.1$  °C/year (p-value=0.8). This is similar to our earlier results as far as statistical significance of mid-cloud temperature trend is concerned. Since there is no new information is obtained by this exercise we are retaining the trends of mid-cloud temperature in the manuscript.

*13. P. 15809 Line 23-25: Do you expect that midlatitude cirrus would have similar trends? I would not expect this because midlatitude clouds are primarily synoptically forced and the dynamic feedbacks might be different in each case. Do you have any thoughts on why optical depth would be decreasing in a warming climate?*

Reply: We agree with the referee that the tropical cirrus clouds differ significantly from the mid-latitude cirrus clouds in terms of their formation mechanism and their properties. However, climate warming is a global issue which will have definite impact on cirrus clouds present at different regions of globe with different magnitudes of changes. Recent climate model simulations done by Chepfer et al., 2014 suggest that in a +4K climate there will be an

upward shift in the cirrus clouds everywhere (including mid-latitude) with the highest shift in the tropics.

As to the second part of this comment, we do not have definite or conclusive thought about why cirrus cloud optical depth should decrease in warming climate. Warming climate pushes up the tropopause altitude and altitude of occurrence of cirrus clouds. Hence, we speculate that this will reduce the cloud physical and optical thickness. Since this statement is highly speculative we have not mentioned in the manuscript.

*14. Figure 1 font sizes are much too small to be legible. Hopefully the final version will be a large portion of the page.*

Reply: As the page dimensions are different for ACPD and ACP article, we hope there will be improvement in the figure for ACP format. At the time of proof-reading, we will try to fix this issue.

Long-term trend analysis and ~~16-year~~ climatology of  
tropical cirrus clouds ~~over a tropical station in southern~~  
~~India~~ using 16 years of lidar dataset over Southern  
~~India~~ ~~ground and space-based lidar observations~~

Amit Kumar Pandit<sup>1</sup>, Harish S. Gadhavi<sup>1</sup>, M. Venkat Ratnam<sup>1</sup>, K. Raghunath<sup>1</sup>, S.  
Vijaya Bhaskara Rao<sup>2</sup>, A. Jayaraman<sup>1</sup>

[1]{National Atmospheric Research Laboratory, Gadanki-517 112, A. P., India}

[2]{Department of Physics, Sri Venkateswara University, Tirupati-517502, A.P., India}

Correspondence to: H. S. Gadhavi (harish@narl.gov.in; harish.gadhavi@gmail.com)

**Abstract**

16-year (1998 – 2013) climatology of cirrus clouds and their macrophysical (base height, top height and geometrical thickness) and optical properties (cloud optical thickness) observed using a ground-based lidar over Gadanki (13.5°N, 79.2°E), India, is presented. The climatology obtained from the ground-based lidar is compared with the climatology obtained from seven and a half years (June 2006 – December 2013) of Cloud-Aerosol LIdar with Orthogonal Polarization (CALIOP) observations. A very good agreement is found between the two climatologies in spite of their opposite viewing geometries and the differences in sampling frequencies. Nearly 50-55% of cirrus clouds were found to possess geometrical thickness less than 2 km. Ground-based lidar is found to detect more number of sub-visible clouds than CALIOP which has implications for global warming studies as sub-visible cirrus clouds have significant positive radiative forcing. Cirrus clouds with mid-cloud temperatures between -50°C to -70°C have a mean geometrical thickness greater than 2 km in contrast to the earlier reported value of 1.7 km. Trend analyses reveal a statistically significant increase in the altitude of sub-visible cirrus clouds which is consistent with the recent climate model simulations. The mid-cloud altitude of sub-visible cirrus clouds is found to be increasing at the rate of 41±21 m/year. Statistically significant decrease in optical thickness of sub-visible and thick cirrus clouds is observed. Also, the fraction of sub-visible cirrus cloud is found to have be-increaseding by 9% -induring the last sixteen years (1998 to 2013) at the cost of

[fraction of thin cirrus clouds which is decreased by 7%. This~~which~~](#) has implications to the temperature and water vapour budget in the tropical tropopause layer. [\\_\\_](#)

## 1 Introduction

Cirrus clouds are ubiquitous, high altitude, thin and wispy cold clouds predominantly consisting of non-spherical ice crystals. They exhibit a very high degree of spatio-temporal variability in their macrophysical, microphysical and optical properties (Liou, 1986; Lynch et al., 2001). These clouds affect the earth's radiation budget through two competing radiative effects viz., albedo effect (by reflecting back the incoming shortwave solar radiation) and green-house effect (by trapping the outgoing long wave terrestrial radiation) (Liou, 2005). The former effect causes cooling while the later causes warming. The magnitude of these radiative effects are strong functions of optical and macrophysical (cloud coverage, altitude, thickness) properties. The optical properties are in turn strong function of microphysical (amount, size, shape and orientation of ice-crystals) properties (Liou, 1986; Liou, 2005). Overall, cirrus clouds are found to have net positive radiative forcing (Chen et al., 2000; Hartmann et al., 1992) at the top of the atmosphere (TOA) and thus they warm the climate system. However, these estimates are based on the International Satellite Cloud Climatology Project (ISCCP) cloud data obtained from passive satellites that do not consider the overlap effect of multi-layered clouds. This overlap effect is the largest source of uncertainty in estimating the long-wave radiative fluxes (Stephens et al., 2004) and cannot be neglected in tropics where the occurrence of multi-layered cirrus clouds is the highest (Nazaryan et al., 2008). This difficulty can be overcome only by using ground and space-based lidars that provide vertical distribution of clouds with opposite viewing geometry.

For decades, the representation of cirrus clouds and their processes in the climate models is found to be challenging, partly owing to the lack of fundamental details of cloud microphysical processes and partly due to the inability to resolve small scale processes in a General Circulation Model (GCM) grid box (Boucher et al., 2013 and references therein). For instance, still the cloud feedback from thin cirrus cloud (which causes net warming) amount is unknown which results in a substantial uncertainty in the climate model predictions. Essentially, this demands highly stable, accurate, precise and long-term observations from ground and space-based lidars to understand the processes and validate the models.

Cirrus clouds that cover about 50% of the globe with highest fraction over the tropics (Stubenrauch et al., 2010, 2013) have strong potential to impact the regional (especially the tropics) and global climate. It is well known that water vapour, low temperature and ice nuclei (for heterogeneous freezing) are the main ingredients needed for the formation of cirrus clouds. Recent research shows that the stratospheric water vapour which mainly comes from the tropical tropopause layer (TTL) has been increasing (Rosenlof et al., 2001; Solomon et al., 2010) and this increase is closely associated with the changes in the tropopause temperature (Randel and Jensen, 2013). In addition to this, aerosols in the TTL, some of which serve as ice-nuclei are increasing (Kulkarni et al., 2008; Vernier et al., 2015) especially during the monsoon season over south-east Asia. Latitudinal changes in the distribution of water vapour, temperature and aerosols will affect the distribution of TTL cirrus clouds (Massie et al., 2013) and ultimately affect the Earth's radiation balance. Thus, it is essential to quantify the properties of TTL cirrus clouds and their dependence on geographic locations, temperature (altitude) and aerosol composition which necessitate long-term observations (Randel and Jensen, 2013).

Several modelling studies have suggested that warming climate will affect cirrus cloud properties such as altitude and thickness (Boucher et al., 2013 and references with-in; Chepfer et al., 2014). Long-term observations of vertically resolved properties of cirrus clouds can help in early detection of climate change or validate climate models.

Despite the continuous efforts made to minimize the uncertainties in cirrus cloud properties at regional and global scales through ground-based, space-based and in-situ observations, regional climatologies of tropical cirrus clouds on the decadal time scale are very few. All these facts strongly encourage us to build a detailed cirrus cloud climatology based on 16 years (1998-2013) of ground-based lidar data and seven and a half years (Jun. 2006 – Dec. 2013) of Cloud-Aerosol Lidar with Orthogonal Polarization (CALIOP) ~~on~~<sup>a</sup>board Cloud-Aerosol Lidar and Infrared Pathfinder Satellite Observations (CALIPSO) data over Gadanki (13.5°N, 79.2°E)– a tropical location in South Asia. Note that CALIOP has a narrow swath and repeat-cycle of the order of 16 days in tropics. It is essential to understand whether such low temporal resolution data captures major cloud variability. Further, there are few advantages and disadvantages of both ground-based and space-borne lidars. While the ground-based (space-borne) lidars have excellent vertical and temporal (spatial) resolutions for obtaining cirrus properties, they suffer from poor spatial (temporal) resolutions. Further, no information on cirrus clouds can be obtained using ground-based lidar during cloudy

conditions while space-borne lidars do not have such restrictions as [they are](#) ~~it is~~ being viewed from the top. Thus, both ground-based and space-borne lidars supplement each other. However, as the two lidars have different viewing geometry and sampling frequency, it is important to investigate whether these factors affect long-term climatology.

In this paper, we report analysis of the 16-year climatology of macrophysical (base height, top height and geometrical thickness) and optical properties (cloud optical thickness) of cirrus clouds observed using ground-based lidar at Gadanki. We compare this climatology with that obtained from CALIOP observations (during 2006-2013). The dependence of cirrus cloud geometrical and optical thickness on mid-cloud temperature is also investigated. In addition to this, we also investigate the long-term trends in the properties of sub-visible, thin and thick cirrus clouds using both ~~the~~ lidars.

## 2 Instruments and data used

### 2.1 NARL lidar

For this study, we have used sixteen years (1998-2013) of data from a ground-based lidar situated at [the](#) National Atmospheric Research Laboratory (NARL), Gadanki (13.5° N, 79.2° E). To the best of our knowledge, this is the longest duration [of a](#) ground-based lidar data set ever used for obtaining cirrus cloud climatology over a tropical station. The detailed site description and system specifications of the lidar (hereafter called NARL lidar) are reported in our earlier study (Pandit et al., 2014). A brief description of [the](#) NARL lidar is presented here. [The](#) NARL lidar is a monostatic biaxial system which transmits Nd: YAG laser pulses of wavelength 532 nm at a rate of 20 Hz (50 Hz since 2007). Each pulse has [a](#) pulse energy of 550 mJ (600 mJ since 2007) and [a](#) pulse duration of 7 ns. The backscattered photons are collected by a Schmidt-Cassegrain telescope attached with two identical orthogonally aligned photomultiplier tubes (PMTs). Photon counts are accumulated in 300 m resolution bins and integrated for four minutes. Lidar data were collected only during the nights that are free from low-level clouds and rain. This limits the observation time during the cloudy nights especially during the summer monsoon season (June-September) when the sky is mostly covered with thick low-level clouds. Lidar profiles were rigorously quality checked based on signal to noise ratio before using them in cirrus cloud statistics. A total of 41,280 profiles qualified for building the cirrus cloud climatology.

## 2.2 CALIPSO cloud products

CALIPSO is an integral part of [the](#) afternoon-train (called A-train) constellation of satellites dedicated to the synergistic observation of aerosols and clouds over the entire globe. Since its launch on 28 April 2006, CALIPSO has been consistently providing high quality vertical distribution of aerosol and cloud properties at unprecedented resolution and accuracy (Young and Vaughan, 2009). This has significantly improved our understanding of aerosols and clouds globally. In order to compare the properties of cirrus clouds obtained from NARL lidar, we have used level-2, 5-km cloud layer and cloud profile (Version 3.01, 3.02 and 3.03) data products obtained from CALIOP ~~on~~board CALIPSO. [Here, the attribute 5-km implies 5 km horizontal resolution along the satellite track at ground level](#) . CALIOP is a near-nadir viewing space-based, dual-wavelength, dual-polarization, three channel elastic backscatter lidar that transmits linearly polarized laser pulses having [an](#) average pulse energy of 110 mJ both at first (1064 nm) and second harmonic (532 nm) wavelengths of Nd: YAG laser (Winker, 2003; Hunt et al., 2009; Winker et al., 2009). The specifications of both NARL lidar and CALIOP are compared in Table 1. The backscattered signal is received by a 1 m diameter telescope with parallel and perpendicularly-polarized channels at 532 nm wavelengths and one parallel channel at 1064 nm.

It is well known that the properties of cirrus clouds exhibit significant spatial and temporal variations (Liou, 1986). In order to obtain the best spatio-temporal concurrent observations with respect to NARL lidar observations, CALIOP overpasses within 50 km radius from Gadanki are considered for the period from June 2006 to December 2013. Both day and night-time data are used for obtaining cirrus cloud climatology near Gadanki. The nearest night-time CALIOP overpass takes place at around 20:33 UTC (02:03 local time) which is about 11 km away from Gadanki whereas the nearest day time CALIOP overpass takes place at around 08:21UTC (13:51 local time) which is about 34 km away from Gadanki. The proximity of CALIOP night-time overpasses to Gadanki provides us a unique opportunity to study the properties of cirrus clouds simultaneously using ground-based and space-borne lidars over a tropical station with opposite viewing geometry. Two such nocturnal observations of cirrus clouds over Gadanki obtained using NARL lidar and CALIOP on 19-20 November 2008 and 03-04 December 2013 are depicted in Figure 1, detailed properties of [them](#) ~~which~~ are presented in the next section. The red circle in the CALIOP vertical feature mask (VFM) in Figure 1 (c) and (h) shows the clouds present in the proximity of Gadanki. Because of the 16 days repeat cycle of CALIOP, at most four overpasses can be obtained in



each month, with two day-time and two -night-time overpasses. During the period from June 2006 to December 2013, a total number of 146 (151) data files are collected during the day (night) in the region selected around Gadanki- ~~which contained Cloud profile data files yielded~~ a total number of 2906 (3022) profiles, out of which 1820 (1876) profiles were day (night) time profiles ([Table S1 in the supporting material](#)).

## 2.3 NCEP FNL air temperature data

For the estimation of extinction coefficient and hence the optical thickness of cirrus cloud layers, pressure and temperature (p-T) profiles over Gadanki during the lidar observation time are required. Since, daily p-T profiles are available only at 12:00 GMT (17:30 local time) over Gadanki from the daily radiosonde launches since 2006, we used six hourly air temperature (at 26 pressure levels) from NCEP FNL 1° x 1° data interpolated from the period of 1999-2013 to have near-simultaneous temperature observations over Gadanki during the lidar observation time. For the year 1998 when no NCEP FNL data are available, monthly mean temperature profiles were used for the estimation of the molecular backscattering coefficient. ~~These~~<sup>is</sup> data ~~were~~<sup>as</sup> obtained from the website <http://rda.ucar.edu/datasets/ds083.2/>. Same temperature profiles are used for finding the relation between the cirrus cloud properties and temperature.

## 3 Methodology

### 3.1 Cirrus cloud detection and percentage occurrence

Cirrus clouds observed using NARL lidar data are detected by using Wavelet Covariance Transform (WCT) method as described in Pandit et al. (2014). ~~We optimized this method to detect very thin as well as multi-layered cirrus clouds.~~ Briefly, the cloud detection algorithm uses Haar wavelet with dilation 3 and altitude dependent threshold. The threshold varying with altitude has benefit of low noise in near range and less false detection at far range. Further to avoid false detection, if raw photon counts at cloud layer are not greater than mean background plus three times the standard deviation then those profiles are excluded. Cloud base and top heights of five different layers can be obtained very accurately using this method. The lowest physical thickness that NARL lidar could detect is 600m. To distinguish cirrus cloud layer from other clouds, we used a temperature threshold. Only those cloud layers with a base temperature below -20 °C (which corresponds to a base height above 8 km) are considered as cirrus cloud layer in this study. Cloud layer boundaries in the attenuated



backscattered signal acquired by CALIOP are detected by a Selective, Iterative Boundary Location (SIBYL) algorithm described in Vaughan et al. (2009). This algorithm finds the aerosol and cloud layers (called features) and detects their boundaries. We have used same temperature criterion as for NARL lidar to identify cirrus clouds in CALIOP data.

To know the effects of cirrus clouds on regional climate, it is very essential to know how frequently these clouds occur over a given region (especially over the tropical regions) during different months and seasons in a year. For this, the percentage occurrence (PO) of cirrus clouds at each altitude bin for both NARL lidar and CALIOP cloud layer data sets are calculated by taking [the](#) ratio of number of profiles with cirrus clouds at that bin to total number of profiles (Pandit et al., 2014).

### 3.2 Macrophysical and thermodynamical properties of cirrus clouds

Macrophysical properties of cirrus clouds viz., cirrus base, top, mid-cloud altitude, geometrical thickness and its distance from the tropopause are obtained from both lidar datasets. Mid-cloud altitude of each cloud layer is taken as mid-point between the base and top altitude for that layer. Base and top altitudes of cloud layers are provided directly in CALIOP 5-km cloud layer data files. The geometrical thickness of cirrus clouds is obtained by subtracting the cirrus base altitude from cirrus top altitude. Distance from the tropopause of each cirrus cloud layer [in case of NARL lidar](#) is obtained by subtracting the cirrus mid-cloud altitude from the tropopause height ~~determined from NCEP~~[provided in the](#) FNL ~~temperature profile~~ data [which uses lapse-rate tropopause definition of WMO](#) ~~in case of NARL lidar. Tropopause altitude is determined as the minimum temperature in the 0 to 20 km altitude region.~~ We have used temperature profiles and tropopause height present in CALIOP cloud data products which are originally derived from GEOS-5 data product provided by [the](#) Global Modelling and Assimilation Office (GMAO).

### 3.3 Optical properties of cirrus clouds

Kaestner's lidar inversion method (Kaestner, 1986) has been used for the retrieval of the extinction coefficient ( $\alpha$ ). The extinction profile integrated between cloud base and the top is used to obtain optical thickness of cirrus cloud layers. Molecular backscattering coefficient at 532 nm wavelength is calculated using the pressure and temperature data obtained from NCEP FNL data. Lidar ratio for cirrus clouds is assumed to be constant with altitude and season with a value of 25 sr following CALIOP extinction retrieval algorithm (Young et al.,

2013; Young and Vaughan, 2009). The effect of multiple scattering which is a function of laser penetration depth, cloud range (or height), receiver field of view (FoV), size and shapes of ice-crystals (Eloranta, 1998) cannot be neglected in the measurement of cirrus cloud properties using a lidar with a receiver FoV of 1 mrad. Several studies (Chen et al., 2002; Chepfer et al., 1999; Hogan, 2006; Sassen and Cho, 1992; Sassen and Comstock, 2001) have suggested different values of multiple scattering correction factor ( $\eta$ ) ranging from 0.1 – 0.9 based on different crystal habits and optical properties of cirrus clouds. In this study, the effect of multiple-scattering is taken care by assuming  $\eta = 0.75$  following Sassen and Cho (1992) and Sassen and Comstock (2001). Sassen and Cho (1992) used telescope with field of view 3 mrad which is comparable to our telescope. Sassen and Comstock (2001) used three different values of  $\eta$  depending on cloud type which are 0.6 to 0.7 for thick clouds, 0.8 for thin clouds and 0.9 for sub-visible cirrus cloud. We have used single value 0.75 for all the cloud types instead. In case of CALIOP, ~~However,~~  $\eta = 0.6$  is being used in CALIOP retrieval algorithm of the extinction coefficient (Young et al., 2013; Young and Vaughan, 2009). The reference altitude used in the retrieval of extinction coefficient is 25 km for NARL lidar.

Optical thickness ( $\tau_{cloud}$ ) of cirrus cloud layer is derived using the expression

$$\tau_{cloud} = \int_{z_b}^{z_t} \alpha(z) dz . \quad (1)$$

Where,  $\alpha(z)$  is the extinction coefficient of a cirrus cloud layer with  $z_b$  and  $z_t$  as a base -and top altitudes, respectively.

For the retrieval of particulate extinction coefficient profiles obtained from the attenuated backscattered data acquired by CALIOP, the fully automated retrieval algorithms called Hybrid Extinction Retrieval Algorithms (HERA) are being used (Young and Vaughan, 2009). Once the features (aerosol and cloud layers) are identified by Scene Classification Algorithm (SCA), their lidar ratio is estimated using the transmission method (Young, 1995). When transmission method fails, initial lidar ratio is assigned based on the feature type, for example lidar ratio of 25 sr is chosen for cirrus clouds. HERA is then invoked to compute the extinction coefficient profiles using the profile solver (Young and Vaughan, 2009), which is then integrated to obtain cloud optical depth. ~~Data product is known as feature optical depth and provided up to 10 layers of clouds.~~ We use the variable named feature optical depth from the CALIOP level-2 data product which provides optical depths for ten cloud layers. Only those features for which Cloud-Aerosol Discrimination (CAD) score lies between 80 and 100

and [are](#) located below  $-20^{\circ}\text{C}$  are considered as cirrus cloud layers. Features with negative values of optical depth are excluded from the statistics of cirrus optical properties. Figure 1 (e) and 1 (j) illustrate two cases where extinction profile of cirrus cloud layer observed on two different nights (20<sup>th</sup> November 2008 and 4<sup>th</sup> December 2013) over Gadanki using NARL lidar is compared with the concurrent extinction profiles obtained from CALIOP cloud profile data. For comparison with [the](#) NARL lidar, we averaged three proximate CALIOP profiles shown by blue asterisks in Figure 1(d) and 1(i). ~~On~~[For](#) both ~~the~~ nights, the base and top altitudes of cirrus cloud layer from NARL lidar and CALIOP show [a](#) very good agreement. [Also, the cloud layer structure on 20<sup>th</sup> November 2008 in both lidars show good similarity.](#) However, the structure of cirrus cloud layer [on 4<sup>th</sup> December 2013](#) and the magnitude of extinction coefficient in both ~~the~~ cases are different which may be due to the spatial inhomogeneity of the cloud structure. This can be seen clearly from the CALIOP vertical feature mask (VFM) for the two nights as shown in Figure 1(c) and 1(h). The various macrophysical and optical properties of cirrus cloud layer observed on these two nights are listed in Table 2. [Overall the extinction coefficients and the cloud optical depths observed using NARL lidar are lower than CALIOP. However, the difference is not same on two nights with 4<sup>th</sup> December 2013 night having larger differences.](#) ~~It can be seen that the optical properties of cirrus cloud layer observed on 20<sup>th</sup> November 2008 from both lidars are comparable with each other. On the contrary, cirrus cloud layer observed on 04<sup>th</sup> December 2013 using both the lidars exhibit differences in their optical properties which can be attributed to the differences in the internal structure of the cloud layer observed by the two lidars.~~

## 4 Results and discussion

### 4.1 Occurrence of cirrus clouds over Gadanki: Climatology

The climatological altitude distribution of PO of cirrus clouds for the entire 16 years (1998-2013) irrespective of sampling time is shown with a dashed black line in Figure 2(a). The PO peaks at 14.5 km with a value of 25%. Altitude distribution of PO based on CALIOP data has relatively broader peak with structures. The altitude of peak PO based on CALIOP data is in good agreement with NARL lidar; however, magnitude of peak PO differ significantly with CALIOP having higher values. To investigate whether the difference in time range (16 years vs. 7.5 years) or time of observation (entire night vs. fixed overpass) is responsible for differences in PO based on NARL lidar and PO based on CALIOP, a subset of entire NARL

lidar data-set for the period 2006-2013 is made. This data subset contains lidar data acquired only during the half an hour time window centred at 02:03 hours (mean local time for CALIOP night-time overpass near Gadanki). The PO of cirrus clouds based on sub-set NARL lidar data is shown with a triple-dotted dashed magenta line in Figure 2(a). The altitude distribution of PO based on subset data has a slightly better agreement with the altitude of peak PO values based on CALIOP. However, the difference in magnitude between the two PO distributions is still large. This can be attributed to the limited NARL lidar observation time during the cloudy nights especially during the monsoon season. For the sake of completeness, the PO distribution for the day-time CALIOP observations (shown by red single dotted-dashed line) is also compared with the other three PO distributions. CALIOP night-time PO distribution is slightly larger than that during day-time at all the altitudes. This difference in PO is consistent with the results reported by Sassen et al. (2009) and Thorsen et al. (2013). This has been attributed to two reasons: one due to the day-night difference in the background noise level present in the backscattered signal from the CALIOP measurement and secondly, due to the day-night differences in cirrus cloud occurrence in tropics. The day-time background noise level present in the backscattered signal from the CALIOP measurement is larger than that during the night-time which prevents the detection of very thin cirrus cloud layers during the day. In addition to this, when the formation of cirrus clouds in tropics is directly or indirectly associated with the development of deep-convective clouds which is quite common in tropics, then the frequency of occurrence of cirrus clouds during night and day will be different ~~peaks over land during the late afternoon and early evening hours~~ (Liu and Zipser, 2008; Sassen et al., 2009). Using Micro-pulse lidar observations over a tropical station Nauru Island (0.52° S, 166.92° E), Comstock et al. (2002, Figure 5 (c)) also found higher occurrence of cirrus clouds during evening and night hours than that during noon hours. ~~Thus, night-time CALIOP observations show the higher occurrence of cirrus clouds than that during the daytime.~~ It is not possible to exactly pin-point which mechanism will be dominant for day and night PO difference at Gadanki with the limited dataset which we have used in this study.

## 4.2 Monthly and seasonal variation in PO of cirrus clouds

The altitude distribution of monthly mean PO of cirrus clouds near Gadanki obtained from the 16 years of NARL lidar data and seven and half years of CALIOP night-time data are shown in Figure 3(a) and 3(b), respectively. Both exhibit enhanced PO in the altitude range

of 9-17 km during May-September owing to the increased convective activities in and around Gadanki. During this period, geometrically and optically thick cirrus clouds occur frequently near Gadanki region ([Sunil Kumar et al., 2003](#); Martins et al., 2011; Pandit et al., 2014; ~~Sunil Kumar et al., 2003~~). The occurrence of multi-layered clouds is also high during this time (not shown here). All these factors are responsible for the spread of the PO distribution of clouds during these months. Here, we have not filtered NARL lidar data for 2 AM half-an-hour time window as very few profiles (less than 50) are available in that window during June-August. The altitude of high PO obtained from both ~~the~~ lidars is found above 14 km (Figure 3 (a & b)) during the months of May-September. The monthly mean base and top altitudes of cirrus clouds (represented by filled red squares and filled pink circles superimposed on the colour contours) obtained from both ~~the~~ lidars are consistent with each other (See Figure 3 (a) and 3 (b)). We also observe a significant fraction of cirrus clouds occurring near and some-times above the ~~cold-point~~ tropopause (shown by brown inverted triangles) during May-September months. This result is in good agreement with the observations of Pan and Munchak (2011, Figure 7). ~~In section 4.1, we noted that the cirrus clouds occur more frequently during night-time than day-time. Figure 3 (c) shows the monthly variation of the night PO minus day PO at different altitude bins, and we find that most of the time the night-time PO is greater than the day-time PO. The strongest diurnal variability is seen in the month of May. It is interesting to note that sometimes especially during September-November the day-time cirrus cloud PO is slightly greater than the night-time PO at altitude bins above 10 km. This is also revealed from Figure 3(d) which shows the percentage of cirrus cloud occurrence (irrespective of altitude) out of total number of observations.~~

The seasonal variation in the altitude distribution of PO of cirrus clouds obtained from three (NARL lidar, CALIOP day and night) data sets is illustrated in Figure 2 (b)-(e). [Number of cloudy and total profiles for each season used for calculating PO for both the datasets is provided in Table S1 in the supporting material.](#) During the winter season (Figure 2 (b)), the PO distribution above 15 km from NARL lidar data shows higher values than that of CALIOP data. The climatological PO (1998-2013) distribution from NARL lidar during the pre-monsoon season shows very good qualitative and quantitative match with the CALIOP night-time PO distribution (Figure 2 (c)). During [the](#) monsoon season (Figure 2 (d)), [the](#) number of lidar observations is the lowest. However, the climatological PO from NARL lidar for monsoon season matches well with the CALIOP PO distributions. ~~Cirrus clouds exhibit significant diurnal variation during the pre-monsoon and monsoon seasons. The CALIOP~~

~~(day time) PO becomes greater than the CALIOP (night time) PO during the post monsoon season similar to what we observe in Figure 3 (e).~~ Overall, we see [a](#) very good consistency between [the](#) two lidar systems in observing the seasonal occurrence of cirrus clouds in-spite of opposite viewing geometry.

### 4.3 Macrophysical and thermodynamic properties of cirrus clouds

The histograms for the macrophysical [properties](#) (cirrus base, top and mid-cloud altitude, distance from ~~the~~ tropopause, [and](#) geometrical thickness) and [the](#) thermodynamical ~~propertyies~~ (mid-cloud temperature) of cirrus clouds are shown in Figure 4 and their statistical details are listed in Table 3. The frequency distribution of cirrus base height from both ~~the~~ lidars show [a](#) good agreement (Figure 4 (a)). The distribution is spread out between 8 and 18 km such that it is difficult to pinpoint the most probable cirrus base altitude. Careful observation and comparison of cirrus base distribution with that reported in Nazaryan et al. (2008, Figure 6 in 20° S - 20° N latitude bands) show that the most probable base altitude lies between 12 and 14 km. Both, NARL lidar and CALIOP histograms show [a nearly](#) one to one correspondence with each other in case of cloud top altitude (Figure 4 (b)) and mid-cloud altitude (Figure 4 (c)). The most probable top-altitude of cirrus clouds observed over Gadanki lies in the altitude range of 15-17 km, which is very close to the tropopause. This is in good agreement with values reported by Comstock et al. (2002) over a tropical island (Nauru Island), who found it to be around 16 km. However, it is little higher than values reported by Seifert et al. (2007) who found it to be in the range 13-15 km over Maldives (another tropical island). Both CALIOP and NARL data in Figure 4 (d) show that cirrus cloud observed over Gadanki lie very close to the tropopause. [About 9%](#) ~~Quite a good number~~ of them are found above the tropopause. CALIOP observations show less number of cases of cirrus clouds above the tropopause. Pan and Munchak, (2011) have shown that fixed sampling time of CALIOP can result in underestimation of cirrus clouds above the tropopause. Most of the time, the mid-cloud temperature is less than -65 °C and found to be as low as -85 °C (Figure 4 (e)). NARL lidar and CALIOP night-time data in Figure 4 (f) show that nearly 50-55% of cirrus clouds observed over Gadanki have a thickness less than 2 km. Though, we observed significant day-night differences in the occurrence of cirrus clouds, the day and night distribution of macrophysical and thermodynamic properties of cirrus clouds do not differ much.



379 The geometrical thickness of cirrus clouds depends on the formation mechanism, cloud  
 380 altitude and cloud-temperature. Figure 5 (a)-(c) show the dependence of geometrical  
 381 thickness on the base altitude of [the](#) cloud ( $z_b$ ). For this, we divided all the cirrus cloud layers  
 382 into three groups based on their occurrence in the different altitude regions. These altitude  
 383 regions are  $8 \text{ km} < z_b < 12 \text{ km}$ ,  $12 \text{ km} < z_b < 15 \text{ km}$  and  $z_b > 15 \text{ km}$ . Clouds of thickness less  
 384 than 2 km occur predominantly in altitude range above 15 km. Our results agree well with the  
 385 results obtained using ground-based lidars at other tropical stations viz. Nauru Island  
 386 (Comstock et al., 2002) and Maldives (Seifert et al., 2007). However, NARL lidar is found to  
 387 have ~~more~~[a larger](#) number of thin clouds in [the](#) altitude range above 15 km than CALIOP  
 388 during night time. Again the comparison of NARL lidar and CALIOP day-time for clouds  
 389 above 15 km is good, although caution is advised by Thorsen et al. (2013) while interpreting  
 390 the day-time cirrus cloud observation using CALIOP which are biased towards the smaller  
 391 geometrical thicknesses. Optical properties of these clouds are discussed in the next sub-  
 392 section.

#### 393 **4.4 Optical properties of cirrus clouds**

394 The distributions of optical thickness of cirrus clouds observed over Gadanki using NARL  
 395 lidar and CALIOP data sets are shown in Figure 6 (a). The optical thickness of cirrus cloud  
 396 layers is binned into intervals of 0.1. We see a high fraction of cirrus clouds with optical  
 397 thickness less than 0.1 in all the three data sets. To further investigate the distribution of  
 398 optical thickness we divide each data set of cirrus clouds into different categories. Based on  
 399 the magnitude of optical thickness, Sassen and Cho (1992) classified cirrus clouds into three  
 400 categories viz. sub-visible cirrus clouds whose optical thickness,  $\tau_{cloud} < 0.03$ ; thin cirrus  
 401 clouds with  $0.03 < \tau_{cloud} < 0.3$  and thick cirrus clouds with  $\tau_{cloud} > 0.3$ . When this classification  
 402 was applied to NARL lidar data set, we find that sub-visible, thin and thick cirrus clouds  
 403 occurred nearly 52% (56% during 2006-2013), 36% (36% during 2006-2013) and 11% (8%  
 404 during 2006-2013) of the total observation time, respectively. Sunil Kumar et al., (2003) have  
 405 also reported the similar high occurrence of sub-visible cirrus using six years of data over  
 406 Gadanki. In contrast, nearly equal occurrence of the three cloud categories i.e. 35% sub-  
 407 visible, 32% thin and 33% thick cirrus clouds is observed in CALIOP data, possibly due to  
 408 inability of CALIOP to detect sub-visible cirrus clouds. It is worth to mention ~~here~~[that about](#)  
 409 the aircraft studies made during Tropical Composition, Clouds, and Climate Coupling (TC4)  
 410 experiment which revealed that more than 50% of sub-visible cirrus cloud ~~of~~[with](#) thicknesses [es](#)

less than 0.01 are unaccounted in the current CALIOP level 2 cloud products (Davis et al., 2010). Martins et al. (2011) also have reported the underestimation of sub-visible cirrus clouds fraction in CALIOP level 2 cloud data products. Frequency distributions for the individual categories are shown in Figure 6 (b)-(d). CALIOP (day) data set shows very few cases of sub-visible cirrus clouds with optical depth less than 0.007 [Figure 6 (b)] whereas night-time observations from NARL lidar and CALIOP show high occurrence of cirrus clouds with optical thickness less than 0.007. This can be explained by the low sensitivity of CALIOP to the day-time cirrus clouds due to the higher background noise than that during night-time. Overall, the distributions of optical thicknesses of cirrus clouds show good agreement between NARL lidar and CALIOP data sets. These distributions are also in good agreement with the findings of Comstock et al. (2002). Figure 6 (d) reveals that NARL lidar sampled smaller number of thick cirrus clouds with  $\tau_{cloud} > 1.5$  as compared to CALIOP. This is possibly due to the lack of NARL lidar observations on cloudy nights and lidar's inability to penetrate the opaque clouds.

The optical thickness of cirrus clouds depends on the formation mechanism, cloud-altitude, cloud-temperature, amount, size, shape and orientation of ice-crystals. To investigate the dependence of cirrus optical properties on altitude, we categorized cirrus cloud optical thickness obtained from each data set into three different classes based on their base altitude in the same way we did for the geometrical thickness in section 4.3 (Figure 5). Each data set confirms the high occurrence of sub-visible cirrus clouds occurring above 15 km (Figure 5 (d)-(f)). In addition to this, we find that the fraction of sub-visible cirrus clouds detected by NARL lidar is higher than that detected by CALIOP.

The distribution of each cirrus cloud type as a function of [the](#) mid-cloud altitude is depicted in Figure 7. We observe that the distribution of sub-visible cirrus clouds from each of the data sets is skewed towards the tropopause (between 16 and 17 km). Most of the sub-visible cirrus clouds (Figure 7 (b)) have their mid-cloud altitude in between 14-17 km with maxima at around 16 km. The distribution of thin cirrus clouds is also similar to the sub-visible cirrus clouds in case of CALIOP data-set but [the](#) NARL lidar has [a](#) peak [in the](#) frequency distribution at lower altitude (14 km) (Figure 7 (c)). Thick cirrus clouds as shown in Figure 7 (d) occur most of the time in the altitude range of 12-14 km which may be of convective origin.

Distribution of geometrical thickness with a bin size of 0.5 km for each cirrus cloud type and for each data set is shown in Figure 8. Most of the sub-visible cirrus clouds are less than 2 km



thick (Figure 8 (b)). CALIOP day-time data shows the high fraction of sub-visible cirrus clouds in the 0-0.5 km bin. The distribution of geometrical thickness for thin clouds obtained from NARL lidar slightly differs from that of CALIOP as shown in Figure 8 (c). In case of [the](#) NARL lidar, the peak of the frequency distribution is at about 2.5 km thickness, whereas in case of CALIOP [the](#) peak of the frequency distribution is at less than 2 km. The geometrical thickness of the majority of thin cirrus clouds is less than 3 km. The flat distribution of geometrical thickness for thick cirrus clouds shown in Figure 8 (d) indicates the diversity in the thickness of cirrus clouds. Night-time distributions from both ~~the~~ lidars agree well for thick clouds. However, the bias of CALIOP day-time observations towards smaller geometrical thicknesses can be seen clearly from Figure 8 (d). [This can be explained by the presence of high solar background noise in the CALIOP day-time observations \(Thorsen et al., 2013\). The detection of true boundaries of cirrus clouds becomes cumbersome in the presence of high background noise especially when there are thick clouds below the cirrus clouds. The 60 m vertical resolution of CALIOP could also be one of the reasons behind the high frequency of clouds in the initial bins \(smaller values\) of geometrical thickness.](#)

#### 4.5 Temperature dependence of cirrus properties

In the previous section it is shown that the geometrical thickness of cirrus clouds has [an](#) altitude dependence. We also found that most of the cirrus clouds occurring above 15 km have a geometrical thickness less than 2 km while clouds below 15 km showed the broader distribution (Figure 5 (a)-(c)). ~~As the geometrical and optical properties of cirrus clouds are dependent on temperature, in this section we~~ We investigate the dependence of geometrical and optical properties of cirrus clouds on temperature [in this section](#). Note that the mid-cloud temperature used in case of NARL lidar dataset is NCEP FNL data whereas in case of CALIOP dataset it is GMAO temperature profile data. ~~Figure 9 (a) shows that the thickness of cirrus clouds increases with decrease in mid-cloud temperature, it peaks at about -60 °C and finally decreases as mid-cloud temperature is further lowered.~~ [Figure 9 \(a\) shows the dependence of geometrical thickness of cirrus clouds on the mid-cloud temperature. The geometrical thickness increases from 1 km to 3.5 km as mid-cloud temperature increases from -90 to -60 °C. For the further increase in temperature from -60 to -20 °C, the geometrical thickness decreases to less than 1 km.](#) A very nice agreement is observed between CALIOP night-time and NARL lidar data. The geometrical thickness of cirrus clouds exhibits large

variation of about 1-5 km in the mid-cloud temperature range of -50 °C to -70 °C with a mean geometrical thickness greater than 2 km. This is in contrast to Sunilkumar and Parameswaran, (2005) who found it to be about 1.7 km over Gadanki. This ~~could be~~ possibly due to the use of temperature profiles based on MST Radar by Sunilkumar and Parameswaran, (2005), which are not as accurate as NCEP FNL data and have lower values compared to CIRA Model temperature profile (Parameswaran et al., 2000). However, difference in temperature profile alone is not sufficient to explain the difference in cloud thickness. Also, the other factors like length of dataset and differences in cloud detection algorithms may have contributed to the observed difference noticed in the two studies. The dependence of geometrical thickness on mid-cloud temperature obtained from CALIOP night-time data is compared with that obtained from CALIOP day-time data and is shown in Figure 9 (b). In the temperature range of -45 °C to -60 °C, the day-time dependence appears to be weaker than the night-time dependence ~~obtained from CALIOP data.~~ This could be due to underestimation of geometrical thickness of clouds during day-time by CALIOP as discussed in previous section.

It is important to know the temperature ranges at which optically different cloud types exist. Figure 10 shows the distribution of mid-cloud temperature for each cirrus types. Both, night-time data sets show that the majority of sub-visible cirrus clouds occur at temperatures lower than -65 °C (Figure 10 (b)). In the temperature range of -60 °C to -80 °C, most of the thin cirrus clouds occur (Figure 10 (c)). The distributions of sub-visible and thin cirrus clouds are skewed towards very low temperature. While most of the thick cirrus clouds occur in the temperature range of -40 °C to -70 °C. The type of cirrus clouds is found to be dependent on different temperature regimes. This is may be mainly due to the differences in the cloud-formation mechanisms for example sub-visible cirrus are formed due to in-situ generation near tropopause height whereas thick cirrus are generally formed by convective outflow at relatively lower heights except during deep/overshooting convections. However, CALIOP day-time data set shows rather a flat temperature dependence for all the categories.

#### 4.6 Long-term trends

In our earlier study (Pandit et al., 2014), we reported 8.4% increase in percentage occurrence of cirrus clouds at 16 km altitude and 0.41 and 0.56 km increase in cloud base and top heights respectively over Gadanki in 16 years. Albeit, the percentage increase of 8.4% was not statistically significant. These findings strengthen the hypothesis that warming climate will

cause an upward shift of cirrus cloud (Boucher et al., 2013; Hartmann and Larson, 2002). Assuming a simple linear temporal relation, the rate of upward shift of the base altitude is found to be about 26 m/year while that of the top altitude is found to be about 35 m/year. Chepfer et al. (2014) have predicted an upward shift in the cirrus cloud altitude in tropics at a typical rate of 20 m/year using multiple climate models. Using six years of CALIOP observations, Zhou et al. (2014) have also showed an increase in the amount and altitude of cirrus clouds in response to the surface warming. Since the trends presented in Pandit et al. (2014) were not separated for cloud types (i.e. sub-visible, thin and thick cirrus clouds) and were presented only for three properties (viz. cloud-base-altitude, cloud-top-altitude and percentage occurrence), therefore, here we investigate long-term trends in mid-cloud altitude, mid-cloud temperature, geometrical thickness and optical thickness of each of these cirrus cloud type using both ~~the~~ lidars. Figure 11 shows the trends in above mentioned properties of sub-visible cirrus clouds. [Trends in these properties for all the three cloud types are provided in Table S2 in supporting material.](#) In the last sixteen years, the monthly mean mid-cloud altitude of sub-visible cirrus clouds is found to be increasing at the rate of  $41 \pm 21$  m/year. The trend is found to be statistically significant (p values 0.05 using Student t-test). CALIOP observations also show an increasing trend in the mid-altitude but found statistically insignificant. As expected from mid-cloud-altitude trend, both ~~the~~ lidars show that the mid-cloud temperature is decreasing, which is found to be statistically insignificant. The geometrical thickness however, does not show a statistically significant trend in any of the lidar observations over Gadanki. This is in contrast to mid-latitude station OHP, France where Hoareau et al. (2013) have found statistically significant increase in geometrical thickness but ~~an~~<sup>the</sup> insignificant trend in cloud-mid-altitude. The optical thickness of sub-visible cirrus clouds obtained from both ~~the~~<sup>L</sup> lidars is found to be decreasing. The trend -  $9.4 \times 10^{-5} \pm 5.5 \times 10^{-5}$  per year in the optical thickness of sub-visible cirrus clouds obtained from NARL Lidar is statistically significant (p value 0.09) while CALIOP trend is statistically insignificant. All the properties found to have statistically insignificant trends for thin and thick cirrus clouds except for one. Thick cirrus cloud shows statistically significant decreasing trend (p value 0.01) [of  \$-1.5 \times 10^{-2} \pm 5.3 \times 10^{-3}\$  per year](#) in cloud optical thickness ([Figure S1 in supporting material](#)). In the latest IPCC report (Boucher et al., 2013), a systematic shift from thick high clouds to thin cirrus clouds or vice-versa is suggested as possible mechanism for cloud-climate feedback, however, at the time of the writing IPCC report, evidence for such systematic shift was not available. In this context, we have investigated trends in the fraction of three cloud types. The fraction of sub-visible cloud type

is found to have statistically significant (p value 0.1) increase of 9.4% over 16 years. The increase is at the cost of decrease in thin cirrus cloud fraction which is decreased by 7.6%. It is worth to quote the future projections of the Coupled Model Inter-Comparison Project Phase 5 (CMIP5) which are presented from 2006-2099 under the Representative Concentration Pathway (RCP) 8.5 scenarios. The projection shows ~~(Kishore et al., 2015)~~ warming trend at 100 hPa over wide region of 60°N-45°S, ~~whereas the warming decreases rapidly and becomes cooling with increase in altitudes~~ by the end of twenty-first century ~~(Kishore et al., 2015)~~. ~~At 100 hPa, these models show t~~The projected increase in temperature ~~by of~~ ~3.27K at the end of the twenty-first century ~~under RCP 8.5 scenarios at 100 hPa. This increase is~~ is partly attributed to the increase of sub-visible cirrus clouds near the tropopause region. These may also have significant implications for cross-tropopause water vapour transport and related global climate variability.

## 5 Summary and conclusions

Using the 16 years of lidar observations from a tropical rural site, climatology of cirrus cloud properties is developed and long-term trends are analysed. The ground-based climatology is also compared with the seven and a half year climatology of cirrus clouds observed using CALIOP. Both ~~the~~ datasets exhibit good agreement with each other. Some of the salient features of cirrus clouds emerged from this climatology are summarized below:

1. Cirrus clouds over Gadanki occur more frequently during night-time than during day time except during September to November when the reverse is true.
2. During the months of May to September, ~~while~~ a significant percentage of cirrus clouds are found to occur near the climatological tropopause, ~~while~~ a ~~few~~ 9% of them are found above the tropopause.
3. About 50-55 % of the cirrus clouds observed over Gadanki have a geometrical thickness less than 2 km.
4. Cirrus clouds that occurred with mid-cloud temperature between -50°C to -70°C have a mean geometrical thickness greater than 2 km in contrast to the value 1.7 km reported by Sunilkumar and Parameswaran, (2005). Most of the sub-visible and thin cirrus clouds occurred with a mid-cloud temperature of less than -60 °C.

- 572 5. Analyses of long-term trends show the following: (a) Among the three types only the  
573 sub-visible cirrus clouds show an increase in their altitude of occurrence. (b) Optical  
574 thickness of sub-visible and thick cirrus clouds ~~s show~~ shows a statistically significant  
575 decreasing trend. (c) A 9.4% increase in sub-visible cirrus cloud fraction and 7.6%  
576 decrease in thin cirrus cloud fraction are found from 1998 to 2013.
- 577 6. ~~The~~ The climatology of the NARL lidar and the CALIOP data shows that the NARL  
578 lidar detects more number of sub-visible cirrus clouds (56% of the total observations)  
579 compared to CALIOP (35% of the total observations) for the overlapping period. This  
580 has implication in global warming studies as sub-visible cirrus clouds have significant  
581 positive radiative forcing and their underestimation will lead to underestimation of the  
582 role of cirrus clouds in global warming.

#### 584 **Acknowledgements:**

585 We thank all the colleagues associated with the operation and maintenance of NARL lidar at  
586 Gadanki since 1998. We also thank NARL data centre for providing lidar data. We  
587 acknowledge the assistance given by NASA Langley Research Centre and UCAR in  
588 providing CALIPSO and NCEP FNL data, respectively. One of the authors (Amit Kumar  
589 Pandit) thanks Department of Space, Government of India for providing research fellowship  
590 to carry out this research.

## 591   **References**

- 592   Boucher, O., Randall, D., Artaxo, P., Bretherton, C., Feingold, G., Forster, P., Kerminen, V.-  
593   M., Kondo, Y., Liao, H., Lohmann, U., Rasch, P., Satheesh, S. K., Sherwood, S., Stevens, B.,  
594   and Zhang, X.-Y.: Clouds and Aerosols, in: *Climate Change 2013: The Physical Science*  
595   Basis. Contribution of Working Group I to the Fifth Assessment Report of the  
596   Intergovernmental Panel on Climate Change, edited by: Stocker, T. F., Qin, D., Plattner, G.-  
597   K., Tignor, M., Allen, S. K., Boschung, J., Nauels, A., Xia, Y., Bex, V., Midgley, P. M.,  
598   Cambridge University Press, Cambridge, United Kingdom and New York, NY, USA, 571-  
599   658, doi: 10.1017/CBO9781107415324.016, 2013.
- 600   Chen, T., Rossow, W. B. and Zhang, Y.: Radiative Effects of Cloud-Type Variations, *J.*  
601   *Clim.*, 13(1), 264–286, doi:10.1175/1520-0442(2000)013<0264:REOCTV>2.0.CO;2, 2000.
- 602   Chen, W.-N., Chiang, C.-W. and Nee, J.-B.: Lidar ratio and depolarization ratio for cirrus  
603   clouds, *Appl Opt*, 41(30), 6470–6476, doi:10.1364/ao.41.006470, 2002.
- 604   Chepfer, H., Pelon, J., Brogniez, G., Flamant, C., Trouillet, V. and Flamant, P. H.: Impact of  
605   cirrus cloud ice crystal shape and size on multiple scattering effects: Application to  
606   spaceborne and airborne backscatter lidar measurements during LITE Mission and E LITE  
607   Campaign, *Geophys. Res. Lett.*, 26(14), 2203–2206, doi:10.1029/1999GL900474, 1999.
- 608   Chepfer, H., Noel, V., Winker, D. and Chiriaco, M.: Where and when will we observe cloud  
609   changes due to climate warming?, *Geophys. Res. Lett.*, 41(23), 2014GL061792,  
610   doi:10.1002/2014GL061792, 2014.
- 611   Comstock, J. M., Ackerman, T. P. and Mace, G. G.: Ground-based lidar and radar remote  
612   sensing of tropical cirrus clouds at Nauru Island: Cloud statistics and radiative impacts, *J.*  
613   *Geophys. Res. Atmospheres*, 107(D23), 4714, doi:10.1029/2002JD002203, 2002.
- 614   Davis, S., Hlavkaet, D., Jensen, E., Rosenlof, K., Yang, Q., Schmidt, S., Borrmann, S., Frey,  
615   W., Lawson, P., Voemel, H., and Bui, T. P.: In situ and lidar observations of tropopause  
616   subvisible cirrus clouds during TC4, *J. Geophys. Res.*, 115, D00J17, doi: 10.1029/  
617   2009JD013093, 2010.
- 618   Eloranta, E.: Practical model for the calculation of multiply scattered lidar returns, *Appl Opt*,  
619   37(12), 2464–2472, doi:10.1364/ao.37.002464, 1998.

620 Hartmann, D. L., Ockert-Bell, M. E. and Michelsen, M. L.: The Effect of Cloud Type on  
 621 Earth's Energy Balance: Global Analysis, *J. Clim.*, 5(11), 1281–1304, doi:10.1175/1520-  
 622 0442(1992)005<1281:TEOCTO>2.0.CO;2, 1992.

623 Hartmann, D. L. and Larson, K.: An important constraint on tropical cloud - climate  
 624 feedback, *Geophys. Res. Lett.*, 29(20), 1951, doi:10.1029/2002GL015835, 2002.

625 Hoareau, C., Keckhut, P., Noel, V., Chepfer, H., and Baray, J.L.: A decadal cirrus clouds  
 626 climatology from ground-based and spaceborne lidars above the south of France (43.9° N–  
 627 5.7° E), *Atmos. Chem. Phys.*, 13, 6951–6963, doi:10.5194/acp-13-6951-2013, 2013.

628 Hogan, R. J.: Fast approximate calculation of multiply scattered lidar returns, *Appl. Opt.*,  
 629 45(23), 5984, doi:10.1364/AO.45.005984, 2006.

630 Hunt, W. H., Winker, D. M., Vaughan, M. A., Powell, K. A., Lucker, P. L. and Weimer, C.:  
 631 CALIPSO lidar description and performance assessment, *J. Atmospheric Ocean. Technol.*,  
 632 26(7), 1214–1228, doi:10.1175/2009JTECHA1223.1, 2009.

633 Kaestner, M.: Lidar inversion with variable backscatter/extinction ratios: comment, *Appl Opt*,  
 634 25(6), 833–835, doi:10.1364/ao.25.000833, 1986.

635 Kishore, P., Ghouse Basha, Venkat Ratnam, M., Isabella Velicogna and Quarda, T. B. M. J.:  
 636 Evaluating CMIP5 models using GPS radio Occultation COSMIC temperature in UTLS  
 637 region, 21<sup>st</sup> century projection and trends, submitted to *Atmos. Chem. Phys.*, 2015.

638 Kulkarni, P., Ramachandran, S., Bhavani Kumar, Y., Narayana Rao, D. and Krishnaiah, M.:  
 639 Features of upper troposphere and lower stratosphere aerosols observed by lidar over  
 640 Gadanki, a tropical Indian station, *J. Geophys. Res. Atmospheres*, 113(D17), D17207,  
 641 doi:10.1029/2007JD009411, 2008.

642 Liou, K.-N.: Influence of Cirrus Clouds on Weather and Climate Processes: A Global  
 643 Perspective, *Mon. Weather Rev.*, 114(6), doi:10.1175/1520-  
 644 0493(1986)114<1167:IOCCOW>2.0.CO;2, 1986.

645 Liou, K. N.: Cirrus clouds and climate in McGraw-Hill Yearbook of Science and  
 646 Technology, 432 pp., 2005.

647 Liu, C. and Zipser, E. J.: Diurnal cycles of precipitation, clouds, and lightning in the tropics  
 648 from 9 years of TRMM observations, *Geophys. Res. Lett.*, 35(4), L04819,  
 649 doi:10.1029/2007GL032437, 2008.

650 Lynch, D. K., Utah, K. S. D. M. U., Center, D. O. C. S. D. M. N. G. S. F. and University, G.  
 651 S. D. A. S. C. S.: Cirrus, Oxford University Press, USA. [online] Available from:  
 652 <http://books.google.co.in/books?id=58v1fg4xeo8C>, 2001.

653 Martins, E., Noel, V. and Chepfer, H.: Properties of cirrus and subvisible cirrus from  
 654 nighttime Cloud-Aerosol Lidar with Orthogonal Polarization (CALIOP), related to  
 655 atmospheric dynamics and water vapor, *J. Geophys. Res. Atmospheres*, 116(D2), D02208,  
 656 doi:10.1029/2010JD014519, 2011.

657 Massie, S. T., Khosravi, R. and Gille, J. C.: A multidecadal study of cirrus in the tropical  
 658 tropopause layer, *J. Geophys. Res. Atmospheres*, 118(14), 7938–7947,  
 659 doi:10.1002/jgrd.50596, 2013.

660 Nazaryan, H., McCormick, M. P. and Menzel, W. P.: Global characterization of cirrus clouds  
 661 using CALIPSO data, *J. Geophys. Res. Atmospheres*, 113(D16), D16211,  
 662 doi:10.1029/2007JD009481, 2008.

663 Pandit, A. K., Gadhavi, H., Ratnam, M. V., Jayaraman, A., Raghunath, K. and Rao, S. V. B.:  
 664 Characteristics of cirrus clouds and tropical tropopause layer: Seasonal variation and long-  
 665 term trends, *J. Atmos. Sol.-Terr. Phys.*, 121, 248-256, doi:10.1016/j.jastp.2014.07.008, 2014.

666 Pan, L. L. and Munchak, L. A.: Relationship of cloud top to the tropopause and jet structure  
 667 from CALIPSO data, *J. Geophys. Res. Atmospheres*, 116(D12), D12201,  
 668 doi:10.1029/2010JD015462, 2011.

669 Parameswaran, K., Sasi, M., Ramkumar, G., Nair, P. R., Deepa, V., Murthy, B., Nayar, S.,  
 670 Revathy, K., Mrudula, G., Satheesan, K., Bhavanikumar, Y., Sivakumar, V., Raghunath, K.,  
 671 Rajendraprasad, T., and Krishnaiah, M.: Altitude profiles of temperature from 4 to 80 km  
 672 over the tropics from MST radar and lidar, *J. Atmos. Sol.-Terr. Phys.*, 62, 1327-1337, doi:  
 673 10.1016/s1364-6826(00)00124-3, 2000.

674 Randel, W. J. and Jensen, E. J.: Physical processes in the tropical tropopause layer and their  
 675 roles in a changing climate, *Nat. Geosci.*, 6(3), 169–176, doi:10.1038/ngeo1733, 2013.

676 Rosenlof, K. H., Oltmans, S. J., Kley, D., Russell, J. M., Chiou, E.-W., Chu, W. P., Johnson,  
 677 D. G., Kelly, K. K., Michelsen, H. A., Nedoluha, G. E., Remsberg, E. E., Toon, G. C. and  
 678 McCormick, M. P.: Stratospheric water vapor increases over the past half-century, *Geophys.*  
 679 *Res. Lett.*, 28(7), 1195–1198, doi:10.1029/2000GL012502, 2001.



680 Sassen, K. and Cho, B. S.: Subvisual-Thin cirrus lidar dataset for satellite verification and  
681 climatological research, *J. Appl. Meteorol.*, 31(11), 1275–1285, doi:10.1175/1520-  
682 0450(1992)031<1275:STCLDF>2.0.CO;2, 1992.

683 Sassen, K. and Comstock, J. M.: A Midlatitude Cirrus Cloud Climatology from the Facility  
684 for Atmospheric Remote Sensing. Part III: Radiative Properties, *J. Atmospheric Sci.*, 58(15),  
685 2113–2127, doi:10.1175/1520-0469(2001)058<2113:AMCCCF>2.0.CO;2, 2001.

686 Sassen, K., Wang, Z. and Liu, D.: Cirrus clouds and deep convection in the tropics: Insights  
687 from CALIPSO and CloudSat, *J. Geophys. Res. Atmospheres*, 114(D4), D00H06,  
688 doi:10.1029/2009JD011916, 2009.

689 Seifert, P., Ansmann, A., Müller, D., Wandinger, U., Althausen, D., Heymsfield, A. J.,  
690 Massie, S. T. and Schmitt, C.: Cirrus optical properties observed with lidar, radiosonde, and  
691 satellite over the tropical Indian Ocean during the aerosol-polluted northeast and clean  
692 maritime southwest monsoon, *J. Geophys. Res. Atmospheres*, 112(D17), D17205,  
693 doi:10.1029/2006JD008352, 2007.

694 Solomon, S., Rosenlof, K. H., Portmann, R. W., Daniel, J. S., Davis, S. M., Sanford, T. J. and  
695 Plattner, G.-K.: Contributions of Stratospheric Water Vapor to Decadal Changes in the Rate  
696 of Global Warming, *Science*, 327(5970), 1219–1223, 2010.

697 Stephens, G. L., Wood, N. B. and Gabriel, P. M.: An Assessment of the Parameterization of  
698 Subgrid-Scale Cloud Effects on Radiative Transfer. Part I: Vertical Overlap, *J. Atmospheric*  
699 *Sci.*, 61(6), 715–732, doi:10.1175/1520-0469(2004)061<0715:AAOTPO>2.0.CO;2, 2004.

700 Stubenrauch, C. J., Cros, S., Guignard, A. and Lamquin, N.: A 6-year global cloud  
701 climatology from the Atmospheric InfraRed Sounder AIRS and a statistical analysis in  
702 synergy with CALIPSO and CloudSat, *Atmospheric Chem. Phys.*, 10(15), 7197–7214,  
703 doi:10.5194/acp-10-7197-2010, 2010.

704 Stubenrauch, C. J., Rossow, W. B., Kinne, S., Ackerman, S., Cesana, G., Chepfer, H., Di  
705 Girolamo, L., Getzewich, B., Guignard, A., Heidinger, A., Maddux, B. C., Menzel, W. P.,  
706 Minnis, P., Pearl, C., Platnick, S., Poulsen, C., Riedi, J., Sun-Mack, S., Walther, A., Winker,  
707 D., Zeng, S. and Zhao, G.: Assessment of Global Cloud Datasets from Satellites: Project and  
708 Database Initiated by the GEWEX Radiation Panel, *Bull. Am. Meteorol. Soc.*, 94(7), 1031–  
709 1049, doi:10.1175/BAMS-D-12-00117.1, 2013.

710 Sunil Kumar, S. V., Parameswaran, K. and Krishna Murthy, B. V.: Lidar observations of  
 711 cirrus cloud near the tropical tropopause: general features, *Atmospheric Res.*, 66(3), 203–227,  
 712 doi:10.1016/S0169-8095(02)00159-X, 2003.

713 Sunilkumar, S. V. and Parameswaran, K.: Temperature dependence of tropical cirrus  
 714 properties and radiative effects, *J. Geophys. Res. Atmospheres*, 110(D13), D13205,  
 715 doi:10.1029/2004JD005426, 2005.

716 Thorsen, T. J., Fu, Q., Comstock, J. M., Sivaraman, C., Vaughan, M. A., Winker, D. M. and  
 717 Turner, D. D.: Macrophysical properties of tropical cirrus clouds from the CALIPSO satellite  
 718 and from ground-based micropulse and Raman lidars, *J. Geophys. Res. Atmospheres*,  
 719 118(16), 9209–9220, doi:10.1002/jgrd.50691, 2013.

720 Vaughan, M. A., Powell, K. A., Winker, D. M., Hostetler, C. A., Kuehn, R. E., Hunt, W. H.,  
 721 Getzewich, B. J., Young, S. A., Liu, Z. and McGill, M. J.: Fully automated detection of cloud  
 722 and aerosol layers in the CALIPSO lidar measurements, *J. Atmospheric Ocean. Technol.*,  
 723 26(10), 2034–2050, doi:10.1175/2009JTECHA1228.1, 2009.

724 Vernier, J.-P., Fairlie, T. D., Natarajan, M., Wienhold, F. G., Bian, J., Martinsson, B. G.,  
 725 Crumeyrolle, S., Thomason, L. W. and Bedka, K.: Increase in upper tropospheric and lower  
 726 stratospheric aerosol levels and its potential connection with Asian Pollution, *J. Geophys.*  
 727 *Res. Atmospheres*, 2014JD022372, doi:10.1002/2014JD022372, 2015.

728 Winker, D. M.: CALIPSO mission: spaceborne lidar for observation of aerosols and clouds |  
 729 (2003) | Winker | Publications | Spie, in *Proc. SPIE , Lidar Remote Sensing for Industry and*  
 730 *Environment Monitoring III*, vol. 4893. [online] Available from:  
 731 <http://spie.org/Publications/Proceedings/Paper/10.1117/12.466539#.U7OSke5RVwE.citeulike>  
 732 e, 2003.

733 Winker, D. M., Vaughan, M. A., Omar, A., Hu, Y., Powell, K. A., Liu, Z., Hunt, W. H. and  
 734 Young, S. A.: Overview of the CALIPSO Mission and CALIOP Data Processing Algorithms,  
 735 *J. Atmospheric Ocean. Technol.*, 26(11), 2310–2323, doi:10.1175/2009JTECHA1281.1,  
 736 2009.

737 Young, S. A.: Analysis of lidar backscatter profiles in optically thin clouds, *Appl. Opt.*,  
 738 34(30), 7019, doi:10.1364/AO.34.007019, 1995.

739 Young, S. A. and Vaughan, M. A.: The Retrieval of Profiles of Particulate Extinction from  
 740 Cloud-Aerosol Lidar Infrared Pathfinder Satellite Observations (CALIPSO) Data: Algorithm

741 Description, J. Atmospheric Ocean. Technol., 26(6), 1105–1119,  
742 doi:10.1175/2008JTECHA1221.1, 2009.

743 Young, S. A., Vaughan, M. A., Kuehn, R. E. and Winker, D. M.: The Retrieval of Profiles of  
744 Particulate Extinction from Cloud–Aerosol Lidar and Infrared Pathfinder Satellite  
745 Observations (CALIPSO) Data: Uncertainty and Error Sensitivity Analyses, J. Atmospheric  
746 Ocean. Technol., 30(3), 395–428, doi:10.1175/JTECH-D-12-00046.1, 2013.

747 Zhou, C., Dessler, A. E., Zelinka, M. D., Yang, P. and Wang, T.: Cirrus feedback on  
748 interannual climate fluctuations, Geophys. Res. Lett., 2014GL062095,  
749 doi:10.1002/2014GL062095, 2014.

750

751

752 Table 1. Specifications of NARL-lidar and CALIOP

Characteristics	NARL lidar	CALIOP
Operating Wavelength(s)	532 nm	532 nm, 1064 nm
Average pulse energy	550 mJ (1998 – 2006) 600 mJ (2007 – 2013)	110 mJ
Pulse width	7 ns	20 ns
Pulse repetition rate	20 Hz (1998 – 2006) 50 Hz (2007 – 2013)	20.16 Hz
Telescope diameter	35.5 cm	100 cm
Receiver field of view	1 mrad	130 $\mu$ rad
Detectors	Photomultiplier Tube (PMT)	PMT for 532 nm Avalanche photodiode for 1064 nm
Polarization	Co and cross-polarized*	Co and cross-polarized for 532 nm Co-polarized for 1064 nm
Vertical resolution	300 m	30 m for altitude range -0.5 to 8.2 km 60 m for altitude range 8.2 to 20.2 km
Horizontal resolution	Stationed	0.333 km for altitude range -0.5 to 8.2 km along the track 1 km for altitude range 8.2 to 20.2 km along the track

\*only co-polarized data of 532 nm channel are used.

753

754 Table 2. Macrophysical and optical properties of cirrus cloud layer detected using NARL  
 755 lidar and CALIOP on 19-20 November 2008 and 3-4 December 2013.

Date	19-20 November 2008		03-04 December 2013	
Characteristics	NARL lidar	CALIOP	NARL lidar	CALIOP
Local Time	02:07:38	02:07:48	Average of 02:02 and 02:06	02:05:00
Cloud base altitude (km)	14.91	14.94	11.62	11.53
Mid-cloud altitude (km)	15.81	15.90	12.67	12.55
Cloud top altitude (km)	16.71	16.86	13.72	13.56
Geometrical thickness (km)	1.80	1.92	2.10	2.03
Tropopause height (km)	16.41	16.66	16.44	16.51
Distance from tropopause (km)	-0.60	-0.76	-3.77	-3.96
Average layer extinction coefficient (1/km)	0.03	0.05	0.53	0.88
Cloud Optical Depth	0.06	0.09	0.11	0.18

756

757 Table 3. Mean, median and standard deviation of macrophysical and thermodynamical  
 758 properties of cirrus clouds obtained from NARL Lidar and CALIOP over Gadanki. Values in  
 759 the parentheses represent the median.

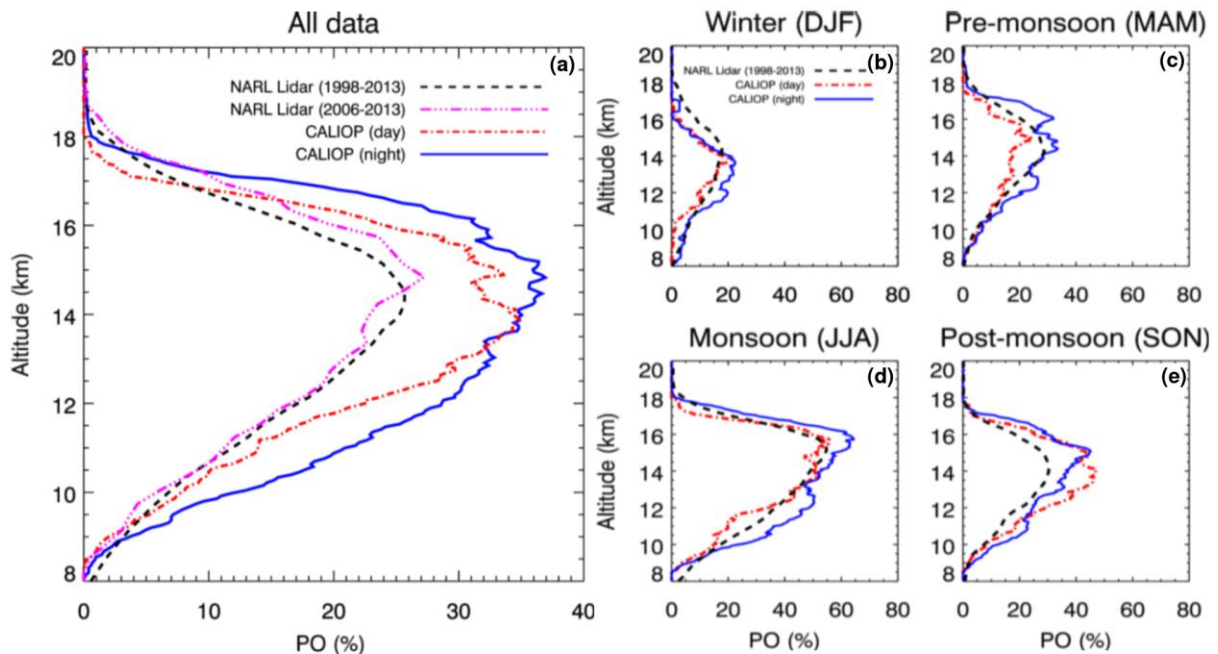
Cirrus Properties	NARL Lidar	CALIOP (night)	CALIOP (day)
Base altitude (km)	$13.0 \pm 2.2$ (13.1)	$12.5 \pm 2.2$ (12.6)	$12.8 \pm 2.0$ (12.7)
Top altitude (km)	$15.3 \pm 2.0$ (15.5)	$14.9 \pm 2.1$ (15.3)	$14.5 \pm 2.0$ (14.9)
Mid-cloud altitude (km)	$14.1 \pm 2.0$ (14.3)	$13.7 \pm 2.0$ (13.9)	$13.6 \pm 1.9$ (13.8)

Geometrical thickness (km)	$2.3 \pm 1.3$ (1.8)	$2.4 \pm 1.7$ (1.8)	$1.7 \pm 1.2$ (1.3)
Mid-cloud temperature (°C)	$-65.0 \pm 11.9$ (-67.6)	$-61.0 \pm 14.7$ (-63.6)	$-60.5 \text{---} \pm \text{---} 14.4$ (-63.2)
Distance from tropopause (km)	$-2.6 \pm 2.1$ (-2.4)	$-2.8 \pm 2.0$ (-2.7)	$-2.8 \pm 1.9$ (-2.5)

---

## 760 Figures

761  
762 **Figure 1.** (a) Night-time evolution of cirrus clouds as a function of altitude observed on 19-  
763 20 November 2008 using NARL Lidar. Colour scale represents the logarithm of the  
764 normalized photon counts. Cirrus base and top altitudes are shown with blue and brown lines,  
765 respectively. Black dashed vertical line shows the CALIPSO overpass time near Gadanki. (b)  
766 Overpass trajectory of CALIPSO (shown by dashed blue line) near Gadanki (shown by filled  
767 red circle). (c) Colours show the vertical feature mask (VFM) along the CALIPSO track as a  
768 function of altitude on 20 November 2008. The red circle shows the clouds sampled near  
769 Gadanki. (d) Overpass trajectory of CALIPSO (dashed blue line) at around 02:07 LT on 20  
770 November 2008 near Gadanki (red plus symbol). Blue asterisks correspond to the proximate  
771 CALIOP profiles used for averaging, (e) Averaged extinction coefficient profiles obtained  
772 from NARL Lidar (dashed red line) and CALIOP (solid blue line). (f) to (j) are same as (a) to  
773 (e) respectively but for the observations on 03-04 December 2013.



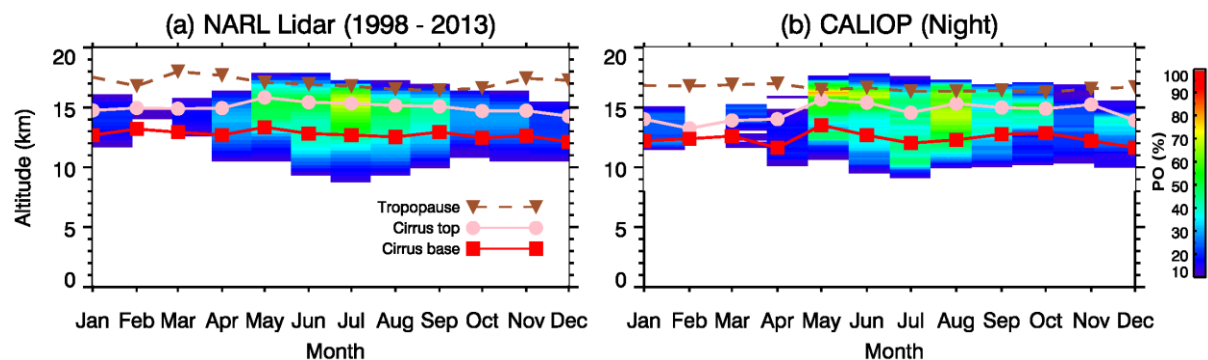
774  
775 **Figure 2.** (a) Climatological altitude distribution of PO of cirrus clouds obtained from  
776 NARL Lidar data for the period 1998-2013 (dashed black line), NARL Lidar data during half  
777 an hour time window centred at 02:03 LT for the period 2006-2013 (triple dotted dashed

778 magenta line), CALIOP day-time (single dotted dashed red line) and CALIOP night-time  
779 (solid blue line) data sets for the period 2006-2013. (b) Same as (a) but for winter (DJF), (c)  
780 pre-monsoon (MAM), (d) monsoon (JJA), and (e) post-monsoon (SON) seasons.

781

782

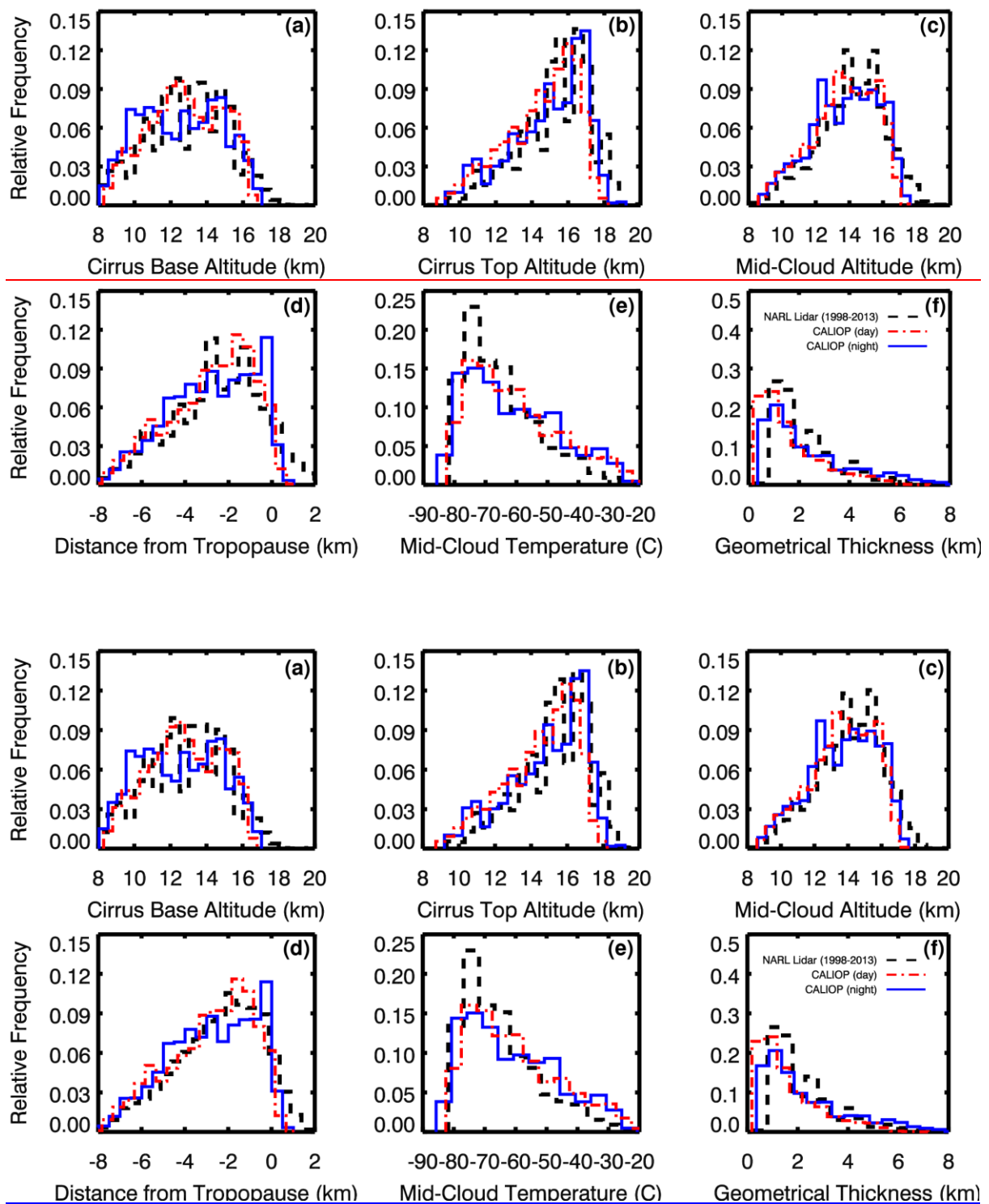




784 Figure 3. Filled contours show the climatological monthly mean variation of PO of cirrus  
785 clouds as a function of altitude over Gadanki (a) during 1998–2013 using NARL Lidar, (b)  
786 during 2006–2013 using CALIOP (night-time) data. Monthly mean tropopause height, cloud  
787 base height and cloud top height are shown by dashed brown lines with inverted triangles, red  
788 line with squares and pink line with filled circles, respectively. ~~(e) Climatological CALIOP~~  
789 ~~night PO minus CALIOP day PO difference as a function of altitude for the period 2006–~~  
790 ~~2013. (d) Monthly PO of cirrus clouds for CALIOP day (solid red line with filled circles) and~~  
791 ~~night (solid blue line with filled circles).~~

792

793



794

795

796

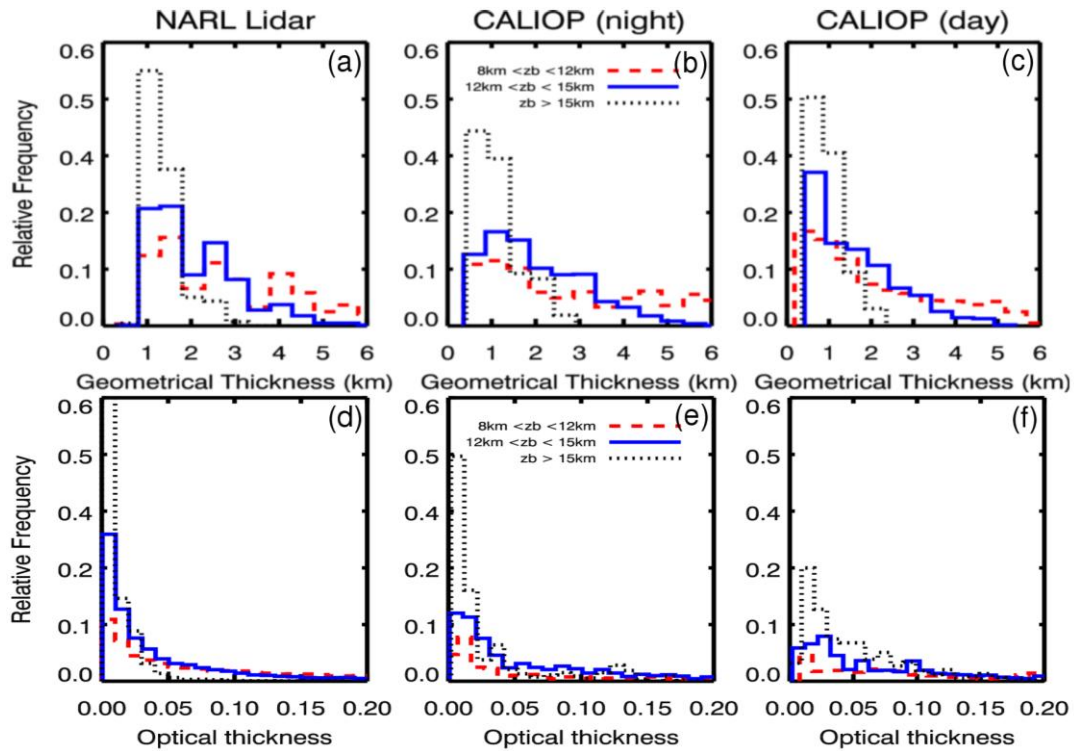
797

798

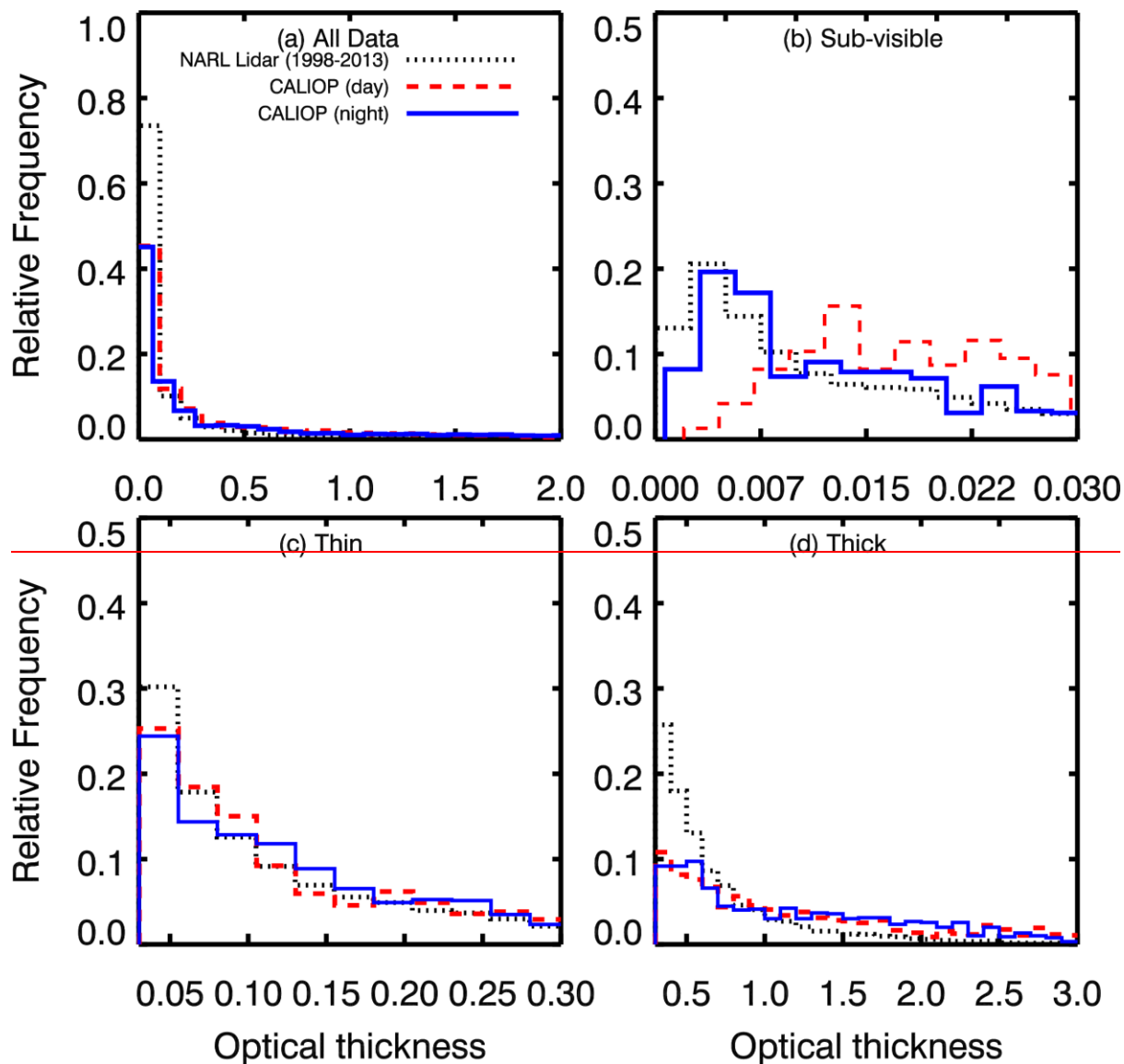
799

**Figure 4.** Histograms showing the [frequency](#) distribution of macrophysical properties of cirrus clouds viz. (a) Base altitude, (b) Top altitude, (c) Mid-cloud altitude, (d) Distance from the tropopause, (e) Mid-cloud temperature, (f) Geometrical thickness obtained from NARL

Lidar (1998-2013) data (dashed black line), CALIOP day-time (single dotted red line) and  
 CALIOP night-time (solid blue line) data sets. Bin size for (a)-(d) and (f) is 0.5 km while bin  
 size for (e) is 5 °C. Tropopause altitude in case of NARL Lidar data is derived from 1° X 1°  
 FNL temperature profile data near Gadanki grid whereas in case of CALIOP data tropopause  
 altitude is derived from GMAO temperature profile data.



**Figure 5.** Histograms showing the frequency distribution of geometrical thickness [(a) to (c)] and optical thickness [(d) to (f)] of cirrus cloud layers with base height ( $z_b$ ) in the ranges of  $8\text{km} < z_b < 12\text{ km}$  (dashed red line),  $12\text{km} < z_b < 15\text{ km}$  (solid blue line) and  $z_b > 15\text{ km}$  (dotted black line) obtained from NARL Lidar data [(a) and (d)] for the period 1998-2013, CALIOP night-time data [(b) and (e)] and CALIOP day-time [(c) and (f)] data sets for the period 2006-2013. Bin size for each histogram of geometrical thickness is 0.5 km while for optical thickness it is 0.01.



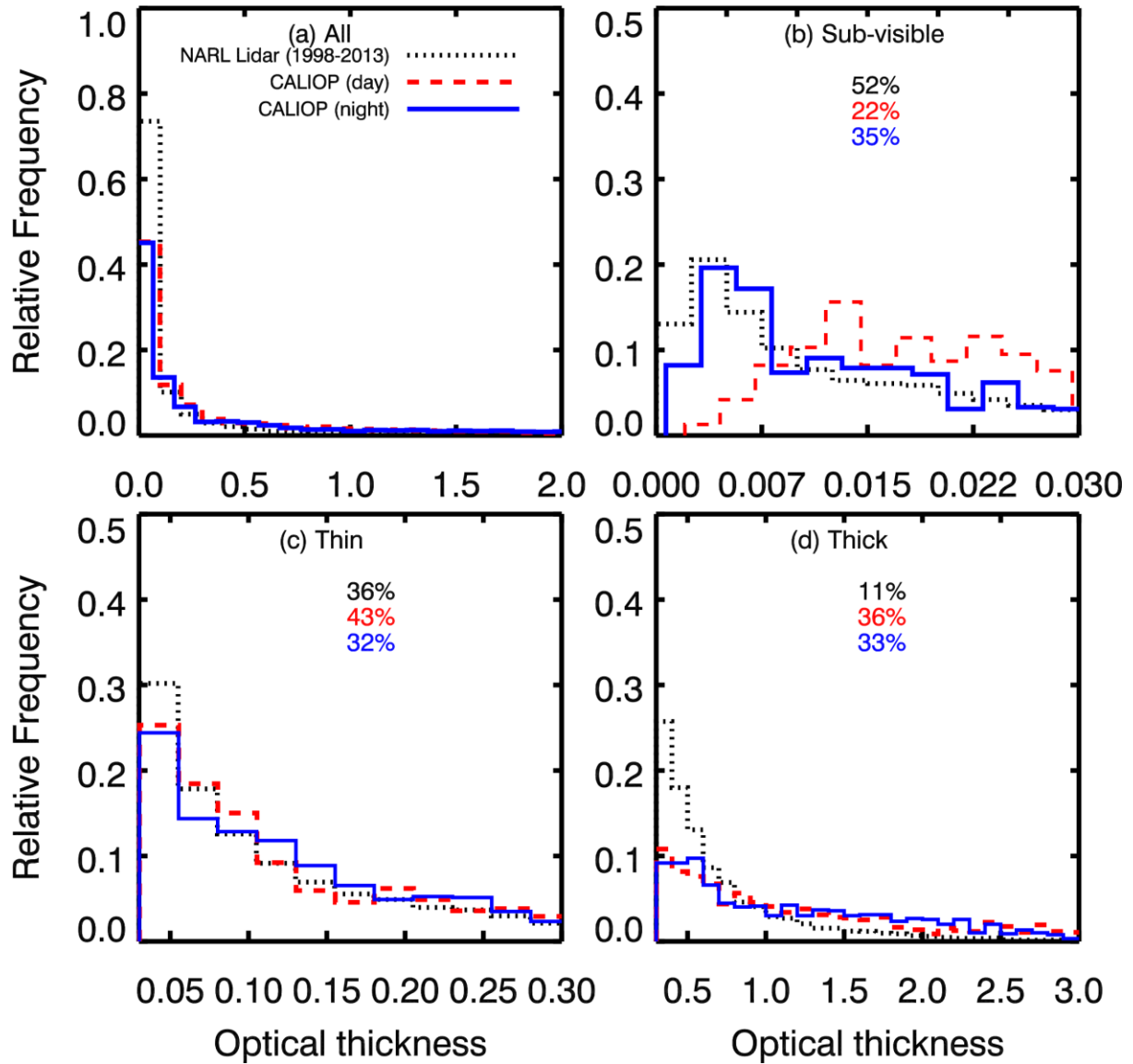


**Figure 6.** Histograms showing the [frequency](#) distribution of optical thickness of (a) all cirrus cloud layers (bin-size = 0.1), (b) sub-visible cirrus ( $\tau < 0.03$ , bin-size = 0.0025), (c) thin cirrus ( $0.03 < \tau < 0.3$ , bin-size = 0.025) and (d) thick cirrus cloud layers ( $\tau > 0.3$ , bin-size = 0.1) obtained from NARL Lidar (dotted black line), CALIOP day-time (dashed red line) and CALIOP night-time (solid blue line) data sets. [Percentage mentioned in each panel is in the same order as legend in \(a\).](#)

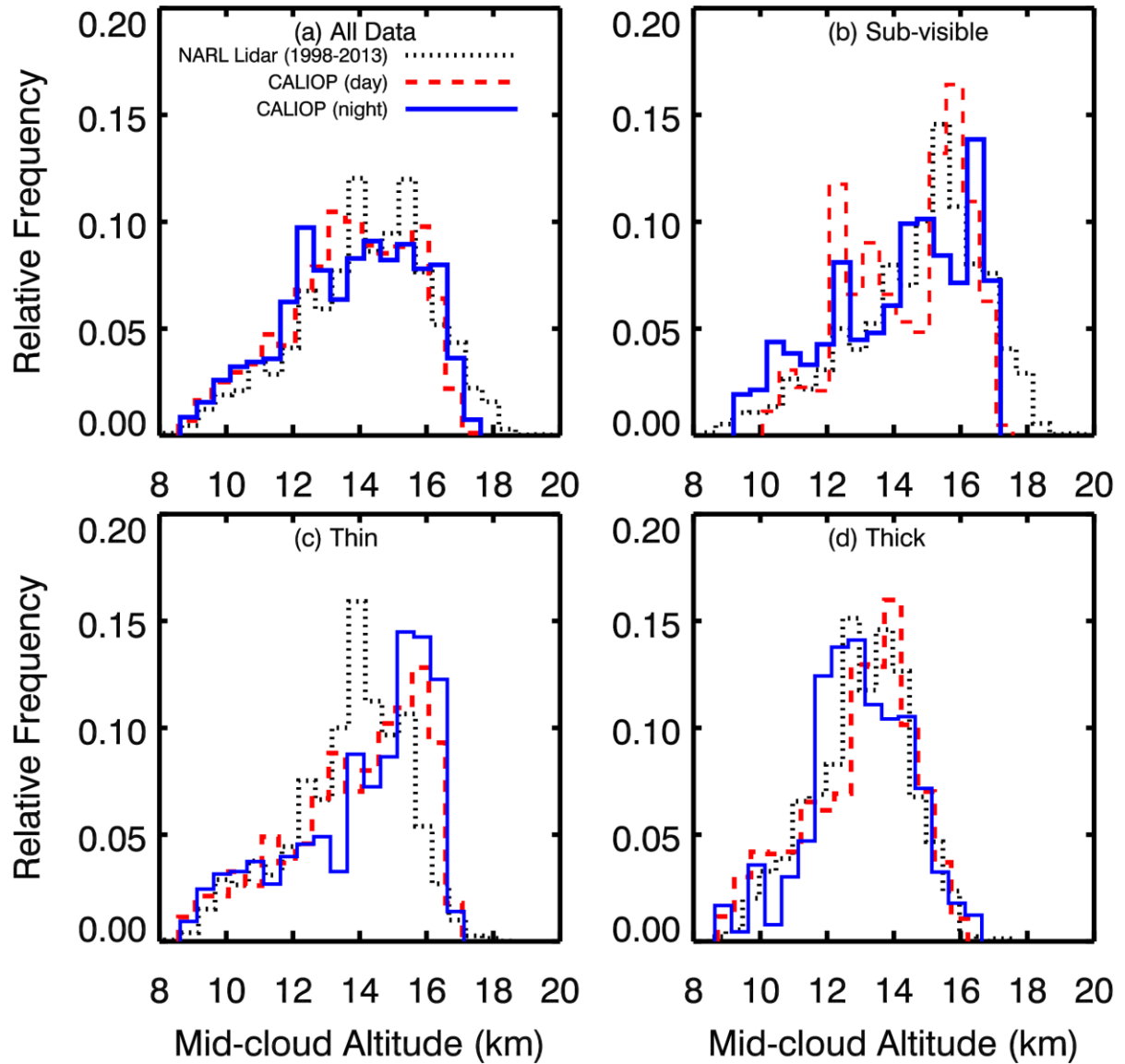


**Figure 7.** Histograms showing the [frequency](#) distribution of mid-cloud altitude in bins of 0.5 km for (a) all cirrus cloud layers, (b) sub-visible cirrus ( $\tau < 0.03$ ), (c) thin cirrus ( $0.03 < \tau < 0.3$ ) and (d) thick cirrus cloud layers ( $\tau > 0.3$ ) obtained from NARL Lidar (dotted black line), CALIOP day-time (dashed red line) and CALIOP night-time (solid blue line) data sets.

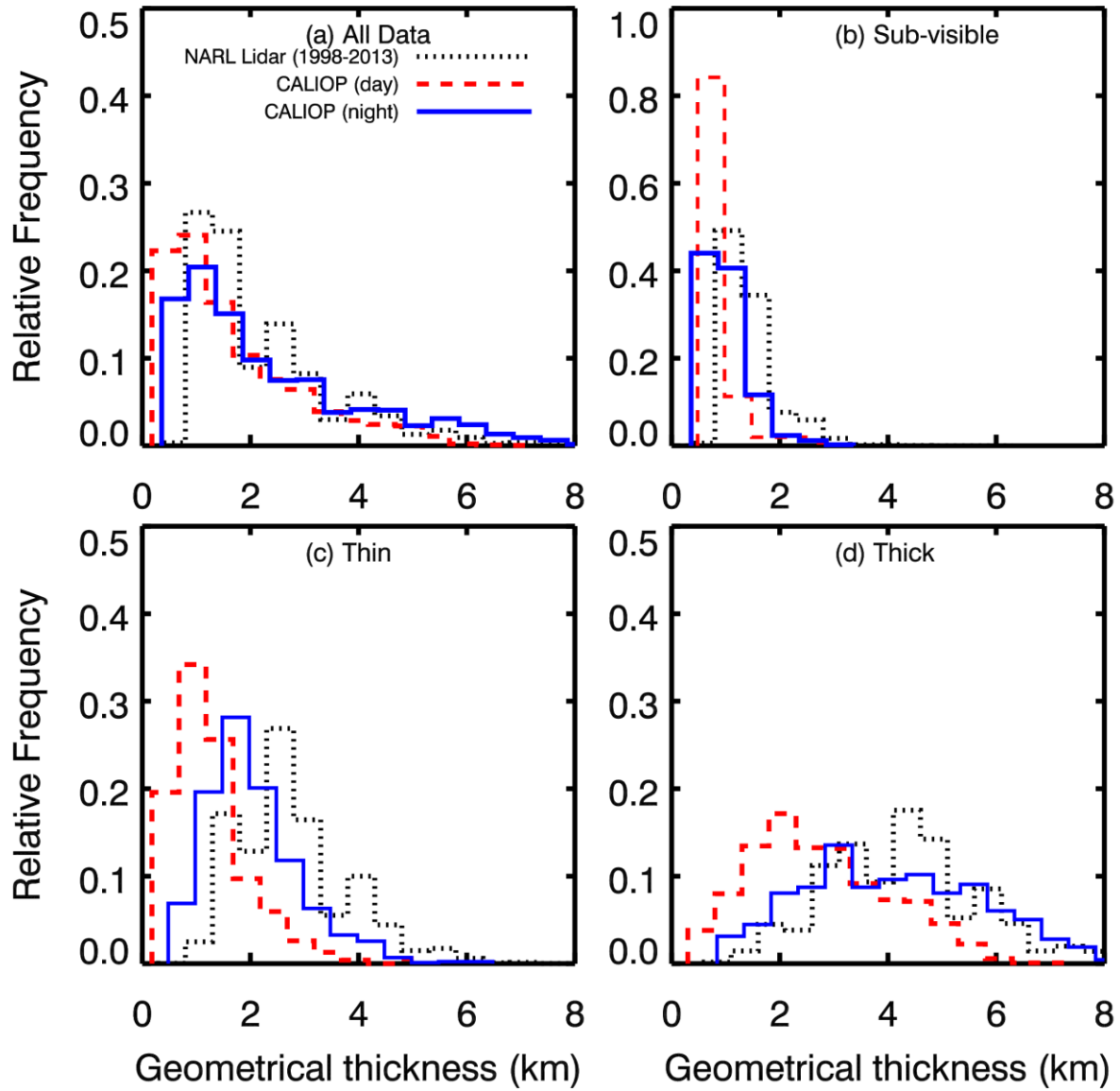


**Figure 8.** Histograms showing the [frequency](#) distribution of geometrical thickness in bins of 0.5 km for (a) all cirrus cloud layers, (b) sub-visible cirrus ( $\tau < 0.03$ ), (c) thin cirrus ( $0.03 < \tau < 0.3$ ) and (d) thick cirrus cloud layers ( $\tau > 0.3$ ) obtained from NARL Lidar (dotted black line), CALIOP day-time (dashed red line) and CALIOP night-time (solid blue line) data sets.

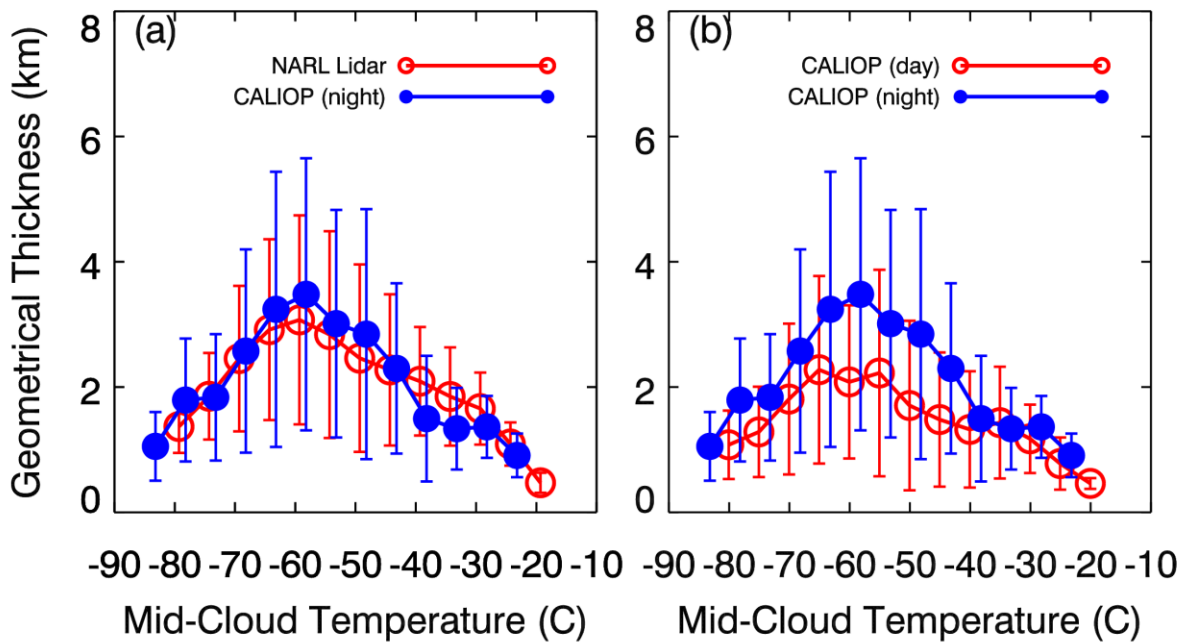


**Figure 9.** Dependence of geometrical thickness of cirrus cloud layers on mid-cloud temperature obtained from (a) NARL Lidar (open red circles) and CALIOP night-time (filled blue circles) data, (b) CALIOP day -time (open red circles) and CALIOP night-time (filled blue circles) data. Circles show the average value while the error bars show the standard deviation.



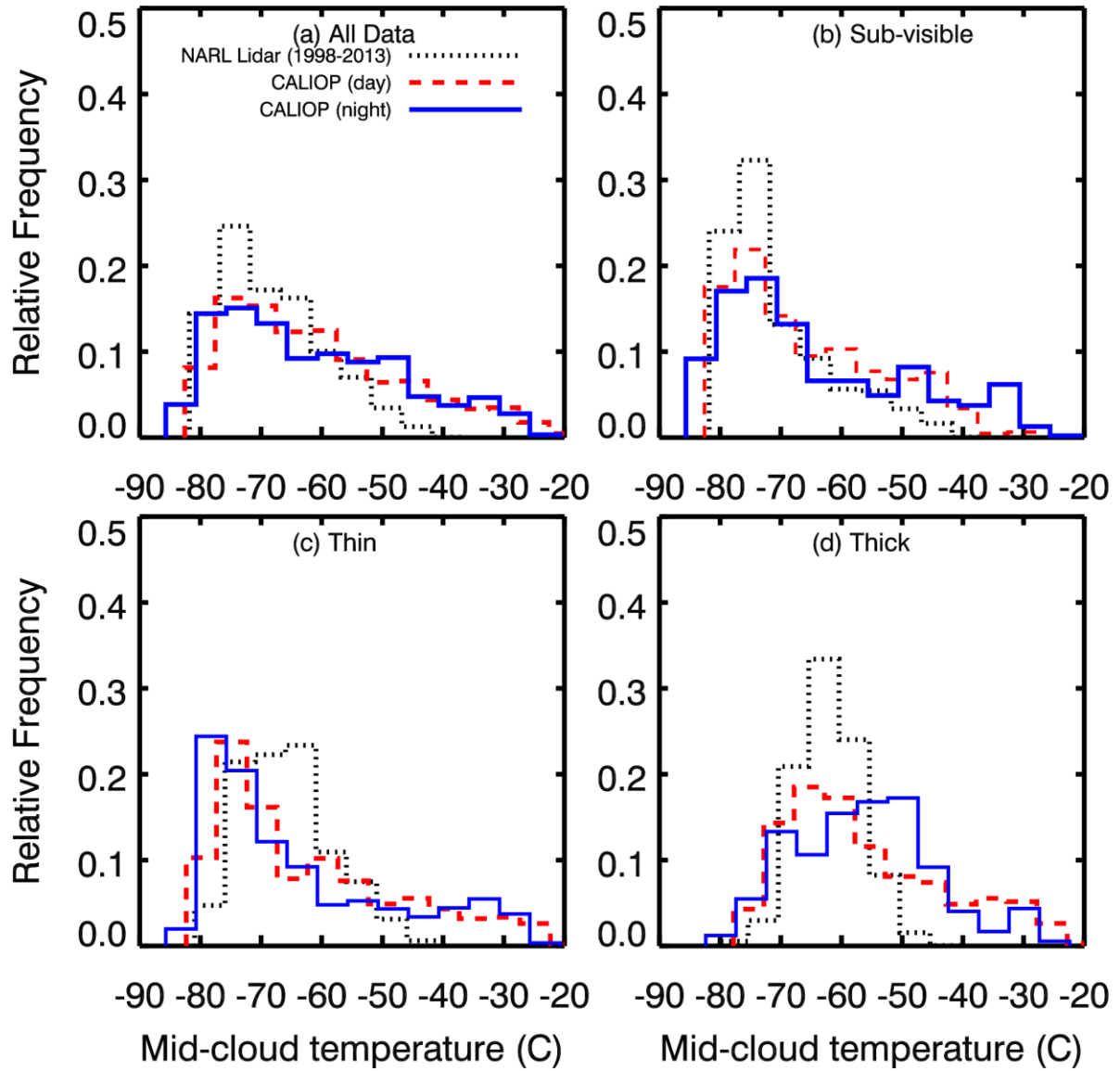


**Figure 10.** Histograms showing the [frequency](#) distribution of mid-cloud temperature in bins of 0.5°C for (a) all cirrus cloud layers, (b) sub-visible cirrus ( $\tau < 0.03$ ), (c) thin cirrus ( $0.03 < \tau < 0.3$ ) and (d) thick cirrus cloud layers ( $\tau > 0.3$ ) obtained from NARL Lidar (dotted black line), CALIOP day-time (dashed red line) and CALIOP night-time (solid blue line) data sets.

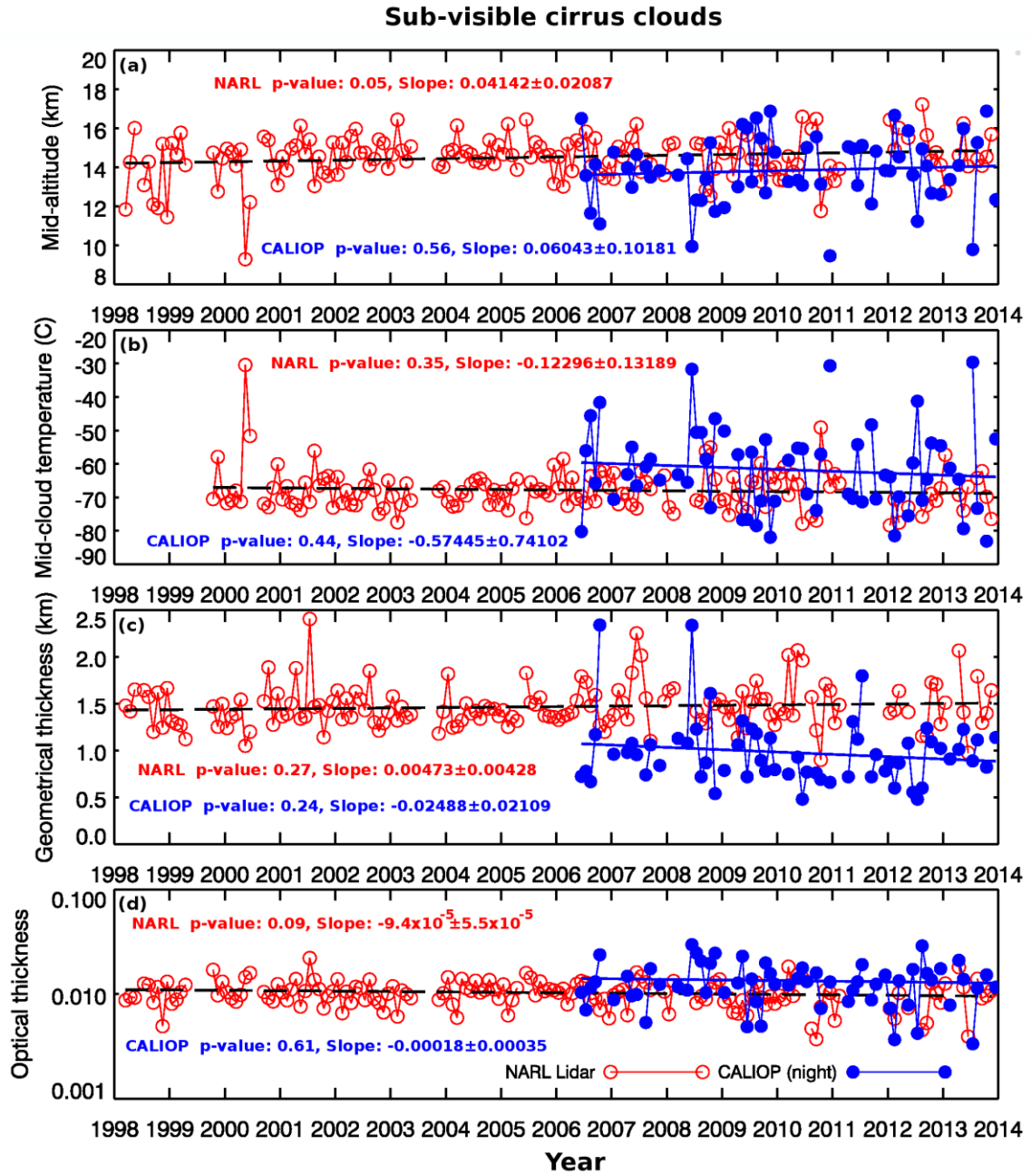


**Figure 11.** Time series of monthly mean (a) mid-cloud altitude, (b) mid-cloud temperature, (c) geometrical thickness and (d) optical thickness of sub-visible cirrus clouds obtained using NARL Lidar (shown by open red circles) and CALIOP night time data (shown by blue filled circle). The dashed black line shows the linear fit to the NARL Lidar data points while the solid blue line shows the same for CALIOP data points. Slopes are expressed in unit per year.